이학박사 학위 논문

Synthesis of melanin nanoparticles and their photosensitizing properties

멜라닌 나노 입자의 합성과 광감성

2016 년 8 월

서울대학교 대학원

화학부 무기화학전공

표 정

Ph. D. Dissertation

Synthesis of melanin nanoparticles and their photosensitizing properties

Supervisor : Professor Dongwhan Lee

Co-supervisor : Professor Jin-Kyu Lee

Major : Inorganic Chemistry

August 2016

By Jung Pyo

Department of Chemistry

The Graduate School

Seoul National University

Abstract

Synthesis of melanin nanoparticles and their photosensitizing properties

Jung Pyo

Department of Chemistry, Inorganic Chemistry

The Graduate School

Seoul National University

Melanins are multifunctional bio-macromolecules found throughout nature, yet they remain as poorly understood class of biomacromolecules compared with other biomolecules such as proteins. Researchers have extensively characterized the molecular building blocks of melanins but their overall architecture has not yet been described. Melanins are categorized chemically into two classes; eumelanin (black) and pheomelanin (red). Although these two types of melanins have common biosynthetic origins, specific molecular reactions occur in the early stage of the synthetic procedure, which differentiate the types of melanin.

The function of melanins is defined by their intriguing physicochemical properties including broadband monotonic absorbance of UV-visible light, extremely low radiative relaxation of photo-excited electronic states, and

powerful anti-oxidant and free radical scavenging abilities. Because of their strong broadband absorption of UV visible light with non-radiative relaxation, melanins have been thought to serve an important photoprotective role and numerous protection-related researches on melanins have been carried out.

In direct contradiction with the photoprotective properties, melanins also show photosensitizing properties upon UV light irradiation. There are some implications of melanins in disease-related events such as photochemistry with the production of DNA strand breaks, suggesting a role of the pigments in carcinogenesis, and neurodegenerative disorders like Parkinson's disease. In this regard, research and establishment of the relationship between structure and physicochemically related biological functions is a starting point in understanding the ambivalent biological behaviors of melanins.

However, the melanin models suggested so far have some limitations such as the lack of solubility in aqueous solutions which is valuable for studying the basic physicochemical properties of melanins and strong binding to proteins in biological environments. In particular, the lack of synthetic method to generate melanin models with their nano-sized particle structure is an intrinsic limitation because the particle characteristic is one of the most prominent features of melanins in nature and a starting point to represent their unique physicochemical properties.

In this thesis, we demonstrated a simple method to synthesize melanin models with nanoparticulate characteristic which have physicochemical properties similar to those of enzyme-synthesized ones. Furthermore, we

examined the photosensitizing function and photo biological function related to chemical components by comparing different types of melanin models. In addition, we examined the oxidation dependent transition of the photo-physical properties of melanins based on the chemical analysis methods of melanins.

Chapter 1 briefly describes the research background of melanins with their structural feature, types and physicochemical properties of natural melanins related to their biological functions and analytical methods by oxidation of melanins.

In chapter 2, we demonstrated a simple method to synthesize pheomelanin nanoparticles (PMNPs) through the polymerization of 3, 4-dihydroxyphenylalanine (DOPA) in the presence of cysteine by $KMnO_4$. The synthesized pheomelanin nanoparticles had a diameter of approximately 100 nm, exhibited high dispersion stability in neutral water and various culture media and possessed morphology similar to that of naturally occurring pheomelanins. The efficiency of photoinduced generation of hydroxyl radicals from PMNPs was determined and related in vitro cell experiments were carried out, with data being compared with those from eumelanin-type nanoparticles (EMNPs) and natural sepia melanin nanoparticles. Endocytosed PMNPs showed the highest phototoxicity (~50% viability) to UV-irradiated HeLa cells, confirming the direct relationship between phototoxic efficiency and the generation of hydroxyl radicals through the complex processes of O_2 sensitization.

In Chapter 3, we assessed the oxidation-dependent photophysical properties of melanins through oxidation of water-dispersible Melanin-like Nanoparticles (MelNps) similar to natural melanins. Oxidation caused an absorption decrement in visible light, increment in the UV region and changes in morphology, especially the oxidation of MelNps with an alkaline hydrogen peroxide environment. The photooxidation of 1, 5-dihydroxynaphthalene (DHN) with singlet oxygen generated by oxidized melanins and direct detection of the singlet oxygen indicated the significant photoreactivity of oxidized melanins. The oxidation of melanins also affected their photoreactivity as well as their efficiency of radical quenching, which was proven through radical quenching experiments.

Keywords: Pheomelanin, Eumelanin, Nanoparticulate structure, water-dispersibility, photosensitization, oxidation-dependent photophysical properties, direct detection of singlet oxygen

Student Number: 2010-23103

Contents

List of Figures

Chapter 1

Chapter 2

Chapter 3

Appendix/Chapter 1

Appendix/Chapter 2

List of Scheme

Chapter 2

Chapter 3

List of Tables

Chapter 2

Chapter 3

Chapter 1

Research Background

1.1. Structure of melanins

The color of skin, hair and eyes mainly depends on the quantity and distribution of melanin pigment. Melanocytes are responsible for the melanogenesis in the melanosomes. Melanocytes in living things produce chemically distinct two types of melanins; black-brownish eumelanin and red-yellowish pheomelanin [1, 2]. Pure eumelanin is found throughout nature, however, pure pheomelanin is not observed in nature and sparsely populated than eumelanin [3]. Eumelanin and pheomelanin are both derived from the common precursor dopaquinone, which is formed following the oxidation of tyrosine by tyrosinase. Figure 1-1 shows the biosynthetic pathways of eumelanin and pheomelanin branch from different reactions involving dopaquinone [4].

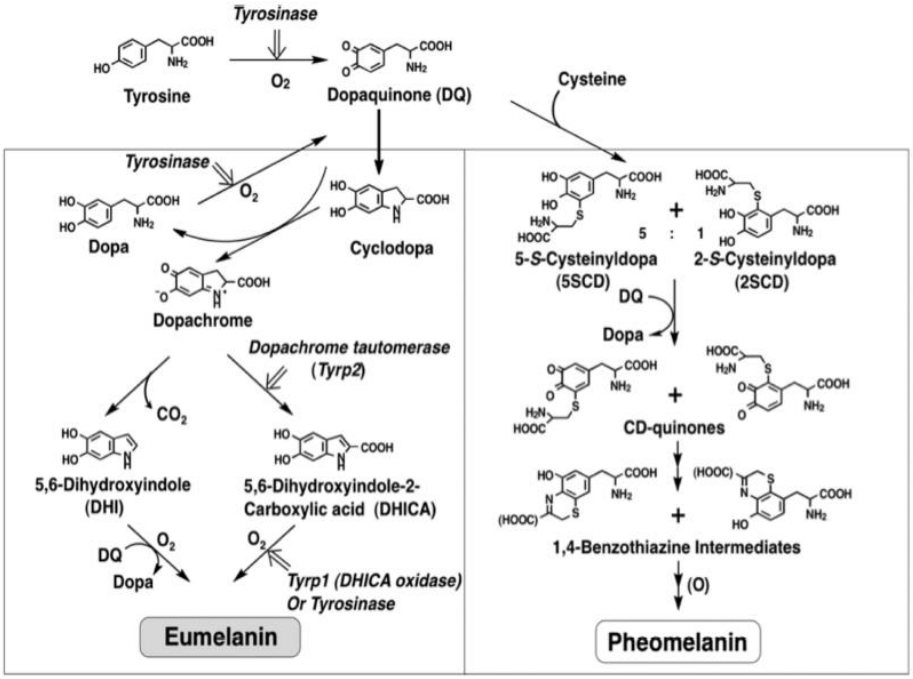

Figure 1-1. Biosynthetic pathways leading to eumelanin and pheomelanin production [4].

Eumelanin is heterogeneous polymer consisting of 5,6-dihydroxyindole (DHI) and 5,6-dihydroxyindole-2-carboxylic acid (DHICA) derived units and pheomelanin consists of sulfur containing of benzothiazine derivatives. The reactive intermediate, dopaquinone, undergoes intramolecular cyclization, leading eventually to the production of eumelanin in the absence of sulfur containing cysteine in the middle of the process. However, in the intervention of cysteine, this process gives rise to the thiol adducts like 5-S-cysteinyldopa (5-S-CD) and 2-S-cysteinyldopa (2-S-CD) leading to the production of pheomelanin [4-6].

Even though it is commonly accepted that eumelanin is composed of DHI

derivatives and pheomelanin is composed of benzothiazine derivatives (figure 1-2), there is no generally accepted secondary model. This is because of the countless of bonding configurations and difficulties in chemical analysis of the assembled macromolecule even from synthetic sources [7].

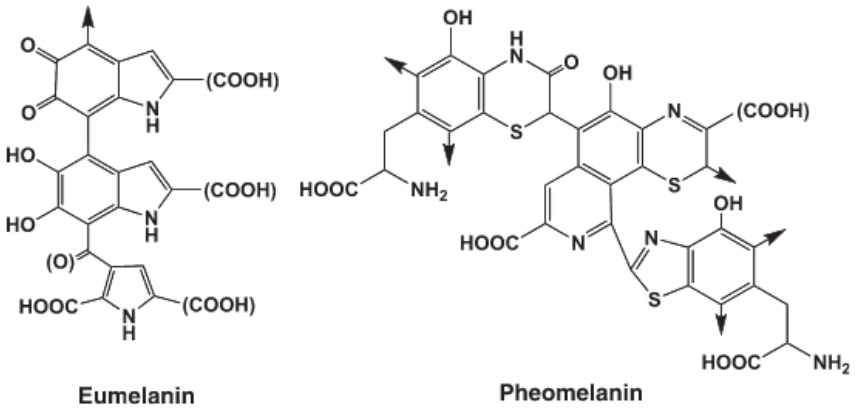

Figure 1-2. Structure of eumelanin and pheomelanin. The positions with (-COOH) in eumelanin structure are connected either to - H or - COOH; these positions may also be available for attachment to other units. The isoquinoline units in pheomelanin structure may be produced by the postpolymerization modification of freshly formed pheomelanin, because these units are not produced in the early stages of pheomelanogenesis [4].

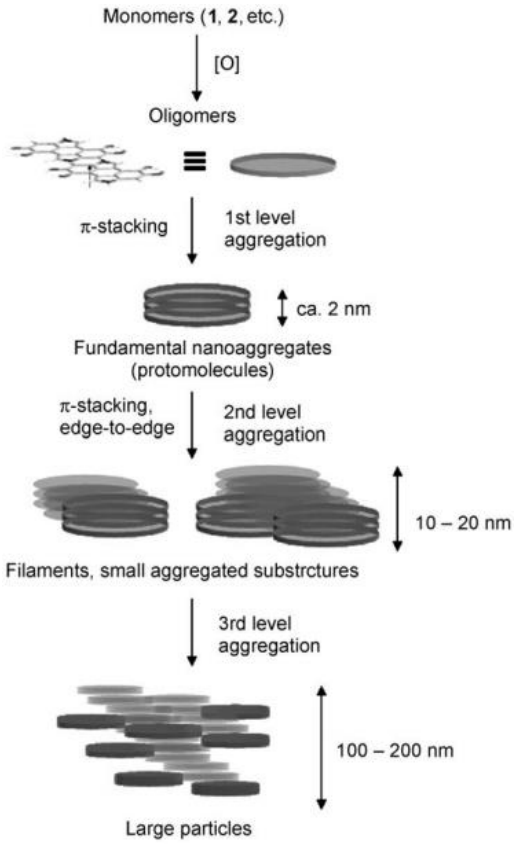

Figure 1-3. The hierarchical aggregate structure proposed for sepia eumelanin [8].

In case of eumelanin, one of the protomolecular structures suggested in mid 1990s is that four or five of planar sheets of four-to-eight 5,6-dihydroxyindole units each stacked along the z section stacking spacing of 3.4 Å in figure 1-3 [9, 10]. Numerous experiments like atomic force microscopy (AFM) [9], NMR spectroscopy [11] and advanced quantum chemical calculations [12] have explained and supported the stacked, aggregation structure of eumelanin, but it is difficult to make definite proof for this model.

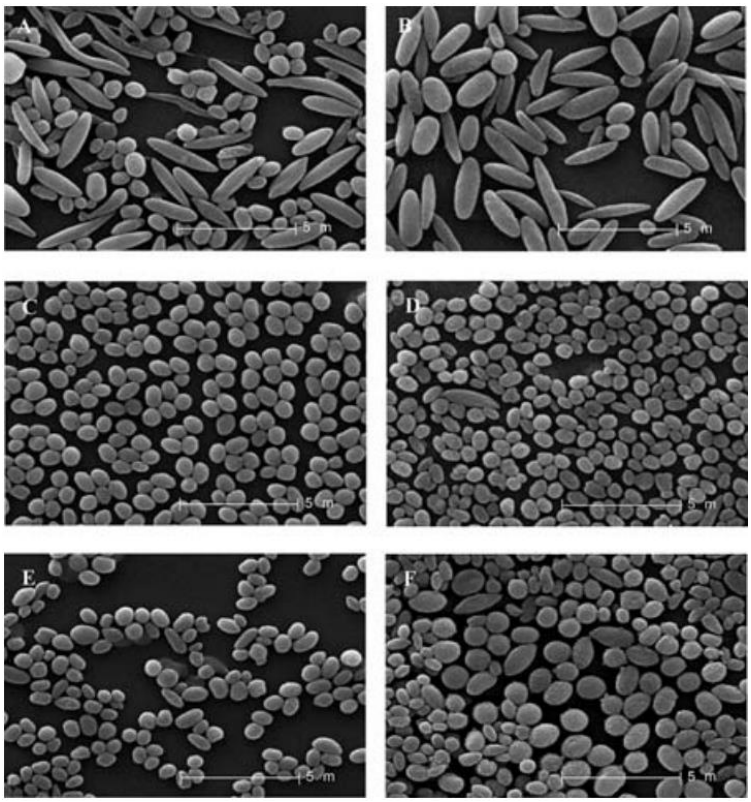

Figure 1-4. . SEM images of (A) adult RPE melanosomes, (B) newborn RPE melanosomes, (C) adult choroid melanosomes, (D) newborn choroid melanosomes, (E) adult iris melanosomes and (F) newborn iris melanosomes [13].

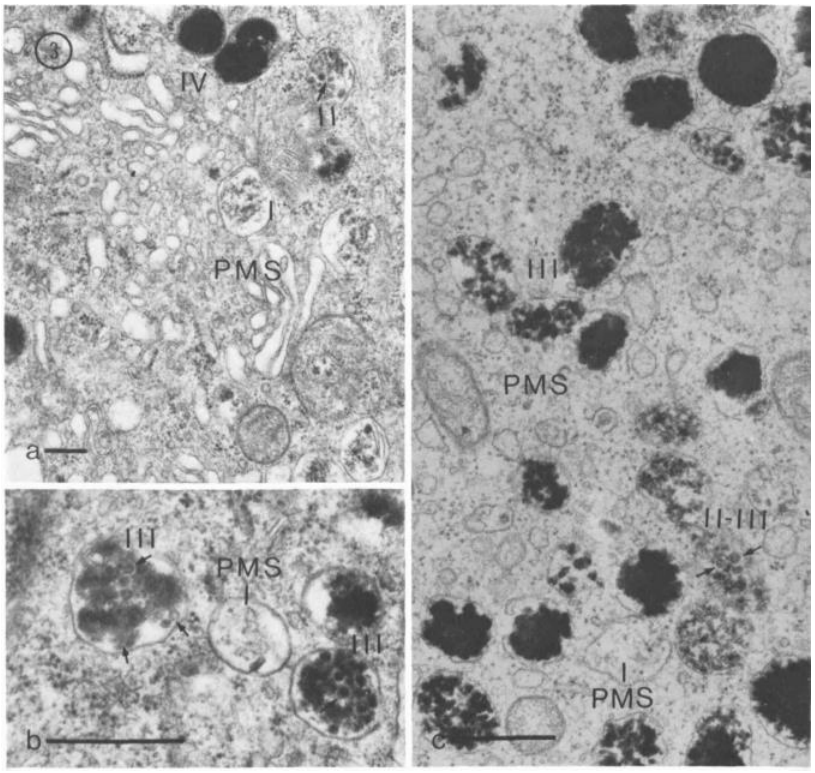

Figure 1-5. Pheomelanosomes (PMS) in hair and feather. a, Yellow hair in agouti mouse. Pheomelanosomes in various stages of differentiation are present. PMS-Ⅱ indicates the pheomelanosome in a late stage Ⅱ. Bar indicates 0.2 μm (x 46000). b, Yellow hair in yellow mouse. A high-power view of pheomelanosomes in stages I and Ⅲ. In stage Ⅲ (PMS-Ⅲ), vesiculo-globular bodies (arrows) fuse with each other, together with amorphous inner material, to form an amorphous matrix. The inner core of these bodies in pheomelanosomes is electron dense as compared with that seen in eumelanosomes. Bar indicates 0.2 μm. (x 146,000). c, Red feather in

Rhode Island Red chick. Again, pheomelanosomes in various stages of differentiation are seen. The ultrastructure of pheomelanosomes and vesiculo-globular bodies (arrows) is essentially similar to that present in yellow hair. Bar indicates 0.2 μm (x 112,000) [14].

Existence as particles sized in nanometer dimension is one of the most prominent features of melanins in nature (Figure 1-4, Figure 1-5). After melanogenesis has been completed, the melanins are packaged into melanosome or pigment granule with diameters of ~ 1 μm which is also consisting of proteins and lipids. The particle character of natural melanins is inherent to their biosynthesis and their chemical structure of melanins [14, 15].

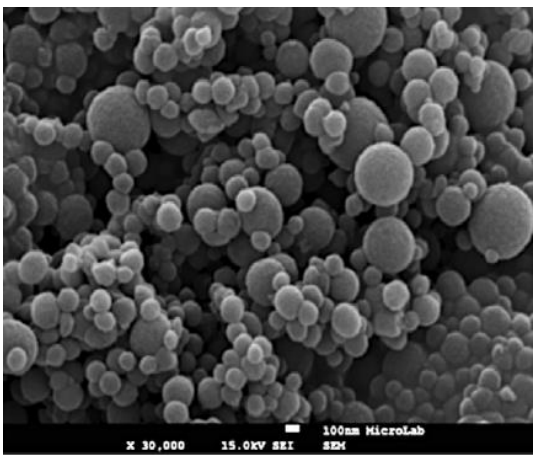

Figure 1-6. SEM image of melanins extracted from cuttlefish [16].

Among synthetic models of melanins, only the polymers that are synthesized by enzymatic method like oxidation of cysteinyl-DOPA and auto oxidation of

DOPA are soluble in aqueous solution at neutral pH [15]. This water solubility of melanins is important to study melanins' physicochemical properties. However, the synthetic models still lacks characteristic particle nature of melanins that requires substantial caution to extrapolate of the properties determined in synthetic models to natural melanins.

1.2. Physical properties of melanins

Broad-band monotonic absorption in the violet and visible region is one of the unique optical properties of melanins [17, 18]. In contrast to most organic systems, there are no distinct chromophoric bands looks more like an inorganic than an organic material [19]. It fits single exponential, the absorbance rises steeply in high energy region that is suitable for function of photoprotection of melanins (figure 1-5).

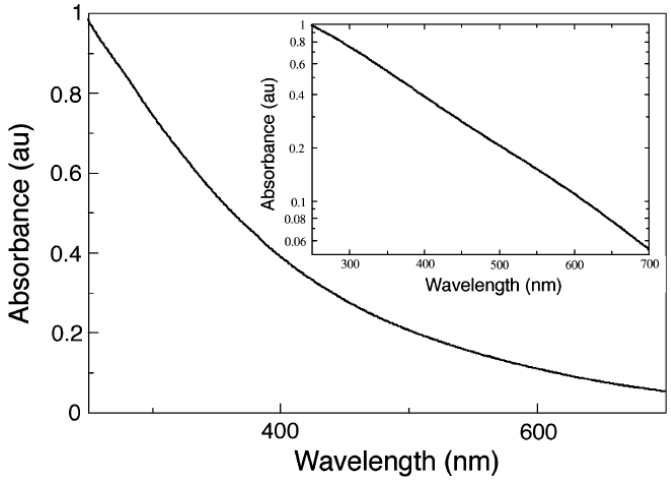

Figure 1-7. The well-known and much reported monotonic, broad band UV-

visible absorption spectrum of eumelanin (synthetic material derived from the non-enzymatic oxidation of dl-DOPA) [18].

Melanins possess a low radiative quantum yield which means that most of all absorbed photons are subject to non-radiative dissipation. As a result of ultrafast photodynamics, energy of the absorbed photons efficiently converted into heat to protect against UV induced DNA damage [20, 21].

Paramagnetic characteristic of melanins is another unusual property. Relatively high concentration of stable free radical compared to other biomacromolecules is detected by electron spin resonance spectroscopy (ESR) signal [22-24].

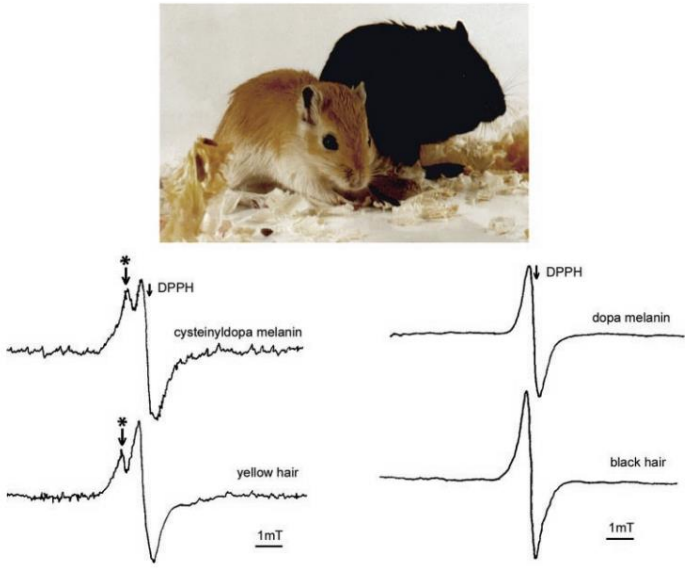

Figure 1-8. ESR analysis of melanin products in follicular melanocytes from

yellow and black gerbils (top). Bottom, left: ESR spectrum of yellow hair showing hyperfine splitting similar to the spectrum of cysteinyl-DOPA melanin (a synthetic model of pheomelanin). Asterisk indicates low field component of the splitting. Bottom, right: EPR signals of black hair and DOPA melanin (a synthetic model of eumelanin with no hyperfine splitting). DPPH, 1,1-diphenyl-2-picrylhydrazyl—the position of a free radical signal (g = 2.0037) [25].

ESR signals of eumelanin are resulted from their semiquinone units. Thus the ESR spectrum of eumelanin corresponds to a slightly asymmetric singlet that generates a free radical signal at approximately g = 2.004 [26, 27]. Whereas, pheomelanin possesses a very distinctive ESR spectrum that is associated with the presence of semiquinonimine.

The concentration of free radicals in melanin is determined by the so-called comproportionation equilibrium which can be affected by a variety of physical and chemical agents. Using ESR spectroscopy, comproportionation equilibrium determines the amount and type of free radicals present in different melanins.

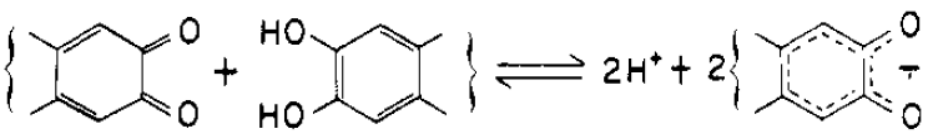

Figure 1-9. The radical equilibrium of eumelanin [27].

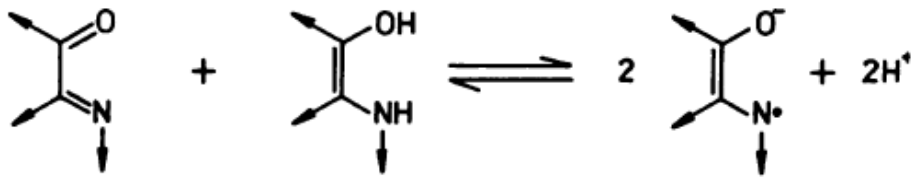

Figure 1-10. The radical equilibrium of pheomelanin.

1.3. Photosensitizing properties of melanins

Melanins are generally thought to absorb UV radication and dissipatation as well as scavenge reactive oxygen radical species to protect nucleus and DNA from UV damage. In contrast to these effects, melanins are known as a photosensitizer that generates reactive oxygen species under UV irradiation.

Photosensitization can proceed via either free radical (type Ⅰ) or singlet oxygen (type Ⅱ) mechanisms. The tyrosine-derived aromatic rings of melanins are excited to the singlet state when they absorb the light, decay to the triplet, and transfer an electron to oxygen to yield superoxide ($O_2^{\cdot-}$). Transfer of excitation from the chromophore to oxygen produces an electronically excited singlet state of oxygen ($^1O_2$) (Figure 1-11). Accordingly, oxygen plays a role in melanin photoreaction that oxygen is consumed during irradiation of melanins.

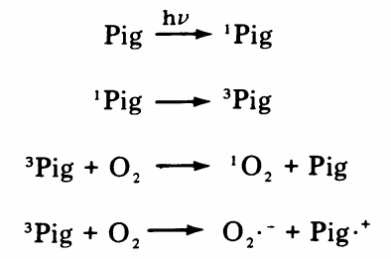

Figure 1-11. Photoreduction of oxygen [28].

There has been an extensive interest in comparing the reactivity of eumelanin of pheomelanin especially in their ability to generate reactive oxygen species [29, 30]. With the study of eumelanin oxygen comsumption occurs as well as the pheomelanin but it is believed that photosensitization is greater for pheomelanin than for eumelanin [31]. Pheomelanin, the red-yellowish pigment, is found in the hair of fair-skinned, red hair humans or red chicken feathers [32, 33] and many available evidences show that fair-skinned humans exhibit a number of abnormal reactions to sunlight, including freckling [34] and a high susceptibility to skin cancer that is linked to greater phototoxicity of pheomelanin [35-37].

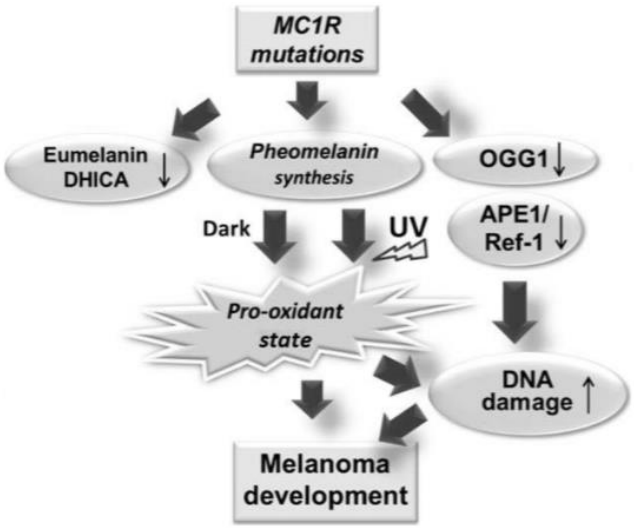

Figure 1-12. Some relationships between the Red Hair Phenotype and melanogenesis [29].

1.4. Oxidation of melanins

Even though there have been a lot of attempts to study melanin structure such as X-ray diffraction and some solid state NMR studies, the current understanding of the molecular structure of melanins has elusive. Many types of melanins have been studied including synthetic and natural pigments which might cause contradictory and some extent the diversity of systems detracted from the development of a basic understanding of structure and function of the natural pigment. In order to study of structure and biological roles of melanin pigments, it is essential to analyze the contents of melanins. To alter their native structure and break them into fragments, chemical treatment that generally involve oxidation procedure of melanins are carried out and specific

degradation products from melanins were also identified (Figure 1-13).

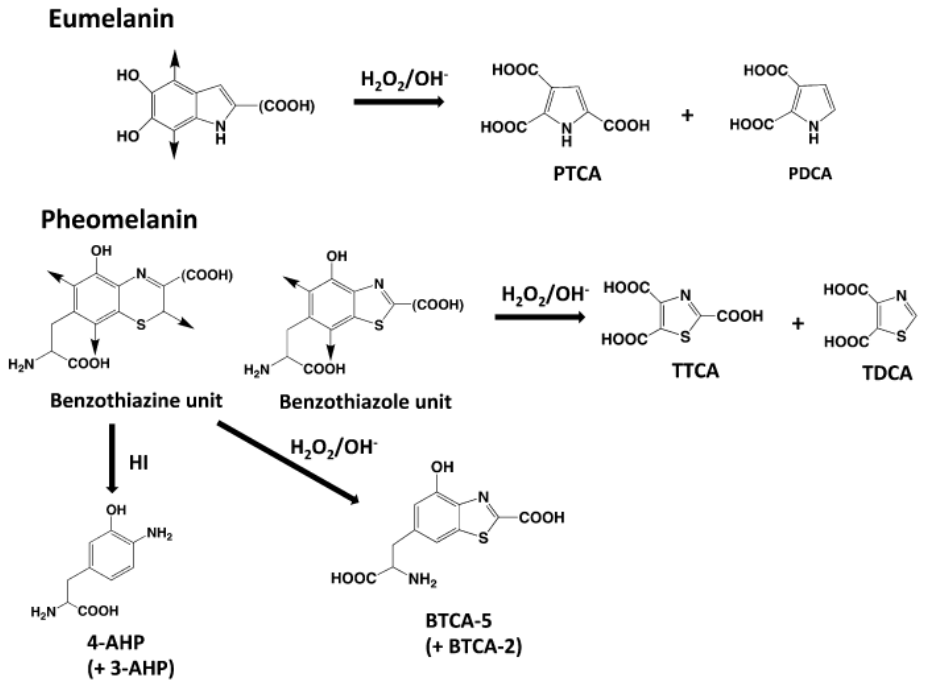

Figure 1-13. Chemical degradation of eumelanin and pheomelanin. Upon H_2O_2 oxidation, DHICA-derived units in eumelanin give PTCA while DHI-derived units gave PDCA. Upon H_2O_2 oxidation, benzothiazole units in pheomelanin give TTCA and TDCA [38].

Oxidation by H_2O_2 to degradation of melanins is also related with the capacity of melanin to scavenge oxidizing species that may be induced by ROS have been of broad interest to many researchers to understand the photophysical properties of melanin and the associated biological functions because H_2O_2 is one of the reactive oxygen species. Melanin oxidation with oxidizing agent such as hydrogen peroxide is one of the most efficient chemicals and has been

extensively studied in solutions because it affects the pigment' s color, morphology and antioxidant behavior of melanins which might have important consequences for the biological functions that might related with the outbreaks of diseases. Moreover, the absorption of melanins significantly decreased in the red end of the spectrum after oxidation, indicating such a change may affects the pigment's photoprotective function.

In cells and organelles, H_2O_2 is an oxidative stress. This is believed to contribute to sight threatening diseases in RPE (retinal pigment epithelium) melanosomes which are sensitive to light exposure [39]. Oxidative stress is also believed to have effects on the skin cancer and neurodegenerative disorder like Parkinson's disease.

1.5. Scope of dissertation

Melanins are one of the most intriguing biopolymers. They have unusual physicochemical properties and diverse biological functions in nature. As a result of their biological significance the melanins have been the subject of intense research, yet they are still remained as poorly understood classes of biomacromolecule compared to other biomolecules such as proteins.

Photoprotection is the generally known function of melanins and numerous protection-related researches of melanins have been carried out. In contrast with the function of photoprotection, the researches for photosensitizing properties of melanins are relatively rare and this photosensitization is greater

for pheomelanin than for eumelanin. However, few studies have been published considering the structure and properties of pheomelanin. Also, comparison between eumelanin and pheomelanin is still difficult because of the appropriate preparation method to synthesis each melanin model to provide similar properties that natural ones have.

Here, we demonstrated the simple method to synthesize water-dispersible pheomelanin nanoparticles which have similar physicochemical properties of enzyme-synthesized ones and have the particle character like pheomelanin in nature. Pheomelanin nanoparticles are appropriate melanin models to compare photosensitizing properties to eumelanin models because they are stable in water and biological medium.

With regard to the photosensitizing properties of melanins, oxidation which induces degradation of melanins has been of broad interest to many researchers to understand the photophysical properties of melanins and the associated biological functions. Melanin oxidation with oxidizing agent affects the pigment' s color, morphology, antioxidant behavior and photophysical properties of melanin which might have important consequences for photoreactivity that might related with the outbreaks of diseases. In this account we demonstrated the change of the photophysical properties of melanins with oxidation.

1.6 Reference

[1] H. S. Raper, The Tyrosinase-tyrosine Reaction: Production from Tyrosine of 5: 6-Dihydroxyindole and 5: 6-Dihydroxyindole-2-carboxylic Acid-the Precursors of Melanin, Biochem. J. 21 (1927) 89–96.

[2] G. Prota, M. Piattelli and R. A. Nicolaus, Preliminary results in the study of phaeomelanins, Rend. Sci. Fis. Mat. 33 (1966) 146–150.

[3] J. D. Simon and D. N. Peles, The red and the black, Acc. Chem. Res. 43 (2010) 1452–1460.

[4] S. Ito, K. Wakamatsu, Chemistry of mixed melanogenesis--pivotal roles of dopaquinone, Photochem. Photobiol. 84 (2008) 582–592.

[5] S. Ito and K. Wakamatsu, Quantitative Analysis of Eumelanin and Pheomelanin in Humans, Mice, and Other Animals: a Comparative Review, Pigm. Cell Res. 16 (2003) 523–531.

[6] K. Wakamatsu and S. Ito, Advanced chemical methods in melanin determination, Pigm. Cell Res. 15 (2002) 174–183.

[7] Y. Liu, V. R. Kempf, J. B. Nofsinger, E. E. Weinert, M. Rudnicki, K. Wakamatsu, S. Ito and J. D. Simon, Comparison of the structural and physical properties of human hair eumelanin following enzymatic or acid/base extraction, Pigm. Cell Res. 16 (2003) 355-365.

[8] M. d'lschia, A. Napolitano, A. Pezzella, P. Meredith and T. Sarna, Chemical and Structural Diversity in Eumelanins: Unexplored Bio-Optoelectronic Materials, Angew. Chem. Int. Ed. Engl. 48 (2009) 3914-3921.

[9] C. M. R. Clancy and J. D. Simon, Ultrastructural Organization of

Eumelanin from Sepia officinalis Measured by Atomic Force Microscopy, Biochemistry 40 (2001) 13353 –13360.

[10] K. C. Littrell, J. M. Gallas, G. W. Zajac and P. Thiyagarajan, Structural Studies of Bleached Melanin by Synchrotron Small-angle X-ray Scattering, Photochem. Photobiol. 77 (2005) 115 – 120.

[11] S. Ghiani, S. Baroni, D. Burgio, G. Digilio, M. Fukuhara, P. Martino, K. Monda, C. Nervi, A. Kiyomine and S. Aime, Characterization of human hair melanin and its degradation products by means of magnetic resonance techniques, Magn. Reson. Chem. 46 (2008) 471 – 479.

[12] K. B. Stark, J. M. Gallas, G. W. Zajac, J. T. Golab, S. Gidanian, T. McIntire and P. J. Farmer, Effect of Stacking and Redox State on Optical Absorption Spectra of Melanins−Comparison of Theoretical and Experimental Results, J. Phys. Chem. B 109 (2005) 1970 – 1977.

[13] Y. Liu, L. Hong, K. Wakamatsu, S. Ito, B. B. Adhyaru, C. Y. Cheng, C. R. Bowers and J. D. Simon, Comparisons of the structural and chemical properties of melanosomes isolated from retinal pigment epithelium, iris and choroid of newborn and mature bovine eyes, Photochem. Photobiol. 81(2005) 510-516.

[14] K. Jimbow, O. Oikawa, S. Sugiyama and T. Takeuchi, Comparison of Eumelanogenesis and Pheomelanogenesis in Retinal and Follicular Melanocytes; Role of Vesculo-globular Bodies in Melanosome Differentiation, J. Invest. Dermatol, 73 (1979) 278–284.

[15] T. Sarna, Properties and function of the ocular melanin—A

photobiophysical view, J. Photochem. Photobiol. 12 (1992) 215-258.

[16] M. Araújo, R. Viveiros, T. R. Correia, V. D. B. Bonifácio and T. Casimiro, Natural melanin: A potential pH-responsive drug release device, Int. J. Pharm. 469 (2014) 140–145.

[17] G. Prota, Melanins and Melanogenesis, Academic Press 1992.

[18] P. Meredith, B. J. Powell, J. Riesz, S. P. Nighswander-Rempel, M. P. Pederson and E. G. Moore, Towards structure–property–function relationships for eumelanin. Soft Matter 2 (2006) 37–44.

[19] M. L. Wolbarsht, A. W. Walsh, and G. George, Melanin, a unique biological absorber, Appl. Opt. 20 (1981) 2184–2186.

[20] E. Kvam and J. Dahle, Pigmented melanocytes are protected against ultraviolet-a-induced membrane damage, J. Invest. Dermatol. 121 (2003) 564–569.

[21] E. Kvam and R. M. Tyrrell, The role of melanin in the induction of oxidative DNA base damage by ultraviolet A irradiation of DNA or melanoma cells, J. Invest. Dermatol. 113 (1999) 209–213.

[22] S. S. Chio, J. S. Hyde and R. C. Sealy, Temperature-Dependent Paramagnetism in Melanin Polymer, Arch. Biochem. Biophys. 199 (1980) 133-139.

[23] R. C. Sealy, J. S. Hyde, C. C. Felix, I. A. Menon and G. Prota, Eumelanins and Pheomelanins: Characterization by Electron Spin Resonance Spectroscopy, Science 217 (1982) 545–547.

[24] R. C. Sealy, J. S. Hyde, C. C. Felix, I. A. Menon, G. Prota, H. M. Swartz,

S Persad and H. F. Haberman, Novel free radical in synthetic and natural pheomelanins: distinction between dopa melanins and cysteinyldopa melanins by ESR spectroscopy. Proc. Natl. Acad. Sci. U.S.A. 1982, 79 (1982) 2885–2889.

[25] P. M. Plonka, A. T. Slominski, S. Pajak and K. Urbanska, Transplantable melanomas in gerbils (Meriones unguiculatus) II: melanogenesis, Exp. Dermatol. 12 (2003) 356–364.

[26] B. Commonner, J. Townsend and G. E. Pake, Free radicals in biological materials. Nature 174 (1954) 689–691.

[27] C. C. Felix, J. S. Hyde, T. Sarna and R. C. Sealy, Interactions of melanin with metal ions. Electron spin resonance evidence for chelate complexes of metal ions with free radicals, J. Am. Chem. Soc. 100 (1978) 3922-3926.

[28] M. R. Chedekel, S. K. Smith, P. W. Post, A. Pokora and D. L. Vessell, Photodestruction of pheomelanin: Role of oxygen, Proc. Natl. Acad. Sci. USA. 75 (1978) 5395–5399.

[29] A. Napolitano, L. Panzella, G. Monfrecola and M. d'Ischia, Pheomelanin-induced oxidative stress: bright and dark chemistry bridging red hair phenotype and melanoma, Pigment Cell Melanoma Res. 27 (2014) 721–733.

[30] T. Sarna and R. C. Sealy, PHOTOINDUCED OXYGEN CONSUMPTION IN MELANIN SYSTEMS. ACTION SPECTRA AND QUANTUM YIELDS FOR EUMELANIN AND SYNTHETIC MELANIN, Photochem. Photobiol. 39 (1984) 69–74.

[31] S. Takeuchi, W. G. Zhang, K. Wakamatsu, S. Ito, V. J. Hearing, K. H.

Kraemer and D. E. Brash, Melanin acts as a potent UVB photosensitizer to cause an atypical mode of cell death in murine skin, P. Natl. Acad. Sci. U.S.A. 101 (2004) 15076-15081.

[32] F. Urbach, J. H. Epstein and P. D. Forbes, Ultraviolet carcinogenesis: Experimental, global and genetic aspects, in: Sunlight and Man, Univ. Tokyo Press, Tokyo (1974) 259-383.

[33] R. H. Thomson, The Pigments of Reddish Hair and Feathers, Angew. Chem. Int. Ed. Eng. 13 (1974) 305- 312.

[34] E. M. Nicholls, Genetic susceptibility and somatic mutation in the production of freckles, birthmarks and moles, Lancet. i (1968) 71-73.

[35] H. O. Lancaster and J. Nelson, Sunlight as a cause of melanoma. A clinical survey, Med. J. Aust. 1 (1957) 452-456.

[36] E. J. MacDonald, The epidemiology of skin cancer J. Invest. Dermatol. 32 (1959) 379-382.

[37] G. T. Pack, J. Davis and A. Oppenheim, The Relation of Race and Complexion to the Incidence of Moels and Melanomas, Ann. N. Y. Acad. Sci. 100 (1963) 719-742.

[38] S. Ito, Y. Nakanishi, R. K. Valenzuela, M. H. Brilliant, L. Kolbe and K. Wakamatsu, Usefulness of alkaline hydrogen peroxide oxidation to analyze eumelanin and pheomelanin in various tissue samples: application to chemical analysis of human hair melanins, Pigment Cell Melanoma Res. 24 (2011) 605–613.

[39] M. Zareba, G. Szewczyk, T. Sarna, L. Hong, J. D. Simon, M. M. Henry

and J. M. Burke, Effects of Photodegradation on the Physical and Antioxidant Properties of Melanosomes Isolated from Retinal Pigment Epithelium, Photochem. Photobiol. 82 (2006) 1024-1029.

Chapter 2

Artificial pheomelanin nanoparticles and their photo-sensitization properties

2.1 Abstract

We demonstrated the simple method to synthesize pheomelanin nanoparticles through polymerization of 3, 4-dihydroxyphenylalanine (DOPA) in the presence of cysteine by $KMnO_4$. The synthesized pheomelanin nanoparticles had a diameter of approximately 100 nm, exhibited high dispersion stability in neutral water and various culture media and possessed similar morphology to naturally occurring pheomelanin. The efficiency of photoinduced generation of hydroxyl radicals from PMNPs was determined and related in vitro cell experiments were carried out, with data being compared to those from eumelanin-type nanoparticles (EMNPs) and natural sepia melanin nanoparticles. Endocytosed PMNPs showed the highest phototoxicity (~50% viability) to UV-irradiated HeLa cells, confirming the direct relationship between phototoxic efficiency and the generation of hydroxyl radicals through the complex processes of the O_2 sensitization.

2.1 Introduction

Melanins are well-known biopolymers that are present in most organisms and play diverse and important roles, including in skin pigmentation [1]. They are used by organisms for, among other things, photosensitization, thermoregulation, radical scavenging, and photoprotection, due to their ability to absorb light throughout the UV and visible regions [2, 3].

Melanins are generally classified either black-brown eumelanin or yellow-red pheomelanin. Eumelanin is believed to result from the oxidation of tyrosine by tyrosinase forming dopaquinone followed by the cyclization to generate 5,6-dihydroxyindole (DHI) and 5,6-dihydroxyindole-2-carboxylic acid (DHICA) and the successive polymerization.4 Meanwhile, pheomelanin derives from benzothiazine units, the compound that results from the incorporation of the sulphur-containing amino acid cysteine into quinones [4,5].

The difference in the structure and physical properties of these two kinds of melanin suggests that they may react differently, both chemically and biologically, when they are exposed to light [6]. For example, while eumelanin acts as a sunscreen against UV radiation, pheomelanin is seemingly more sensitive to radiation and may in fact add to the harmful effects of radiation exposure, including in the formation of carcinoma [7-10]. Differences in chemical composition of various types of melanins can result in different responses to UV excitation. Such excitation is often thermally dispersed, but may also trigger the generation of reactive oxygen species

(ROS), including superoxide and hydroxyl radicals, through catalysed oxygen reduction. This can induce single strand breaks in DNA [7, 11]. Pheomelanin is more efficient at producing oxyradicals than eumelanin [12, 13]. Therefore, it is very important to precisely understand the relationship of the structures of different melanins with their corresponding biological function.

Unfortunately, melanins are difficult to study given their strong binding to proteins in biological environments [14]. Melanins have traditionally either been extracted from organisms in which it occurs naturally or synthesized artificially using a method that mimics biosynthetic pathways. Unfortunately, biological extraction generally requires the repetitive use of strong acids and bases, with no standardized method having been established that leaves the structure intact [14, 15]. Meanwhile, synthetic techniques, which generally involve the chemical or enzymatic oxidation of the necessary precursors, tend to result in structures that lack the necessary particle characteristics of naturally produced melanins [16, 17]. The study is further complicated by the dispersibility of melanins in most solvents, including neutral water, a problem that has been imperfectly addressed through the use of non-biological aqueous alkaline environments [18, 19].

Herein, we report a facile synthetic method by which to prepare pheomelanin-type nanoparticles (PMNPs) with high dispersion stability in both water and biological media. Various properties of the prepared PMNPs were investigated by comparing them with eumelanin-type nanoparticles (EMNPs), which had already been successfully synthesized by our group and

which had also exhibited excellent dispersion stability [20], as well as with natural sepia melanins, so as to determine the differences in photophysical properties that derive from the altered structural composition.

2.2 Experimental Section

Chemicals and characterization

3,4-dihydroxyphenylalanine (DOPA) and L-cysteine were purchased from Sigma-Aldrich, while disodium terephthalate (TA) was purchased from TCI. 1.0 N $KMnO_4$ was purchased from Dae-Jung and dibasic/monobasic buffer solutions of potassium phosphate were purchased from Samchun. WST-1 solution (2-(4-nitrophenyl)-5-(2-sulfophenyl)-3-[4-(4-sulfo-phenylazo)-2-sulfophenyl]-2H-tetrazolium disodium salt) was purchased from Daeil Science. All of these chemicals were used without any further purification. The size and shape of the PMNPs and EMNPs were determined by Transmission Electron Microscopy (TEM, Hitachi 7600) and Electrophoretic Light Scattering Spectrophotometry (ELS -8000). Chemical compositions were measured by Elemental Analysis (Flash EA 1112). UV-Vis spectra were recorded on a SCINCO S-3100 spectrometry. The Electron Spin Resonance (ESR) spectra of PMNPs were recorded using a JEOL JES-TE200 spectrometer.

Synthesis of water-dispersable PMNPs

DOPA (70 mg, 0.35 mol) was dissolved in deionized water (50 mL) with heating, given its poor solubility in neutral water. L-cysteine (85.6 mg, 0.70 mol) was then added at room temperature, after which $KMnO_4$ (360 μL, 1.0 N solution) was added and the solution was stirred vigorously. The solution changed from pale yellow to deep yellow-orange as soon as $KMnO_4$ was

added; after 3 h, it had turned dark brown. The reaction was allowed to continue for an additional 21 h, after which PMNPs were collected by centrifugation (18,000 rpm). To the redispersed solution of PMNPs, HCl (1 mL of 1.0 N) was dropped to remove Mn^{2+} ions and washed three times with deionized water by centrifugation until pH value reached to 7. Any large aggregated PMNPs during the washing processes were removed by centrifugation at low speed (4000 rpm), while the final purified PMNPs were stored in deionized water (~67% yield based on the weight of DOPA).

Preparation of pheomelanin by enzymatic oxidation using tyrosinase

Enzymatic preparation of pheomelanin was accomplished using a known method [23]. DOPA (70 mg, 0.35 mol) was added to 50 mL of a 0.1 M phosphate buffer solution with a measured pH of 6.8 at 37 ℃. L-cysteine (85.6 mg, 0.70 mol) was then added to this solution. After dissolution was complete, tyrosinase (10 mg) was added. The solution developed pink and proceeded to turn brown after 5 h. This reaction continued for 24 h, after which it was quenched by addition of concentrated HCl so as to adjust to a pH of 1.5. The precipitate was collected by centrifugation (4000 rpm) and washed several times with diluted HCl solution (pH 1.5). The product was stored in deionized water.

Isolation and purification of sepia melanins

Ink sacks separated from Korean cuttlefish were incised to extract sepia as mentioned in previously report [27]. After several washing processes of centrifugation and redispersion in deionized water, clean sepia melanins were obtained. Prepared sepia melanins were stored in water and repurified by centrifugation prior to experimentation.

Preparation of EMNPs

DOPA (70 mg, 0.35 mol) was dissolved in 50 mL of deionized water with heating. $KMnO_4$ (0.36 mL, 1.0 N) was then added to the DOPA solution, and the solution turned black several min later [20]. The reaction continued for 24 h, after which the black product was purified by centrifugation (18,000 rpm) and redispersed in water three times. The purified product was stored in deionized water.

Assay for photoreactive properties of melanin NPs

The solutions of dispersed melanin NPs (100 μg/ml, 50 μL, PMNPs or EMNPs) were mixed with deionized water (1.55 ml) in a quartz cuvette. Freshly prepared TA solution (400 μL, 20 mM) was then added to the solution, and the cuvette was capped to prevent solvent loss. The sample was then irradiated by a xenon lamp at a distance of 15 cm for a total of 2 h. Fluorescence intensities from the generated hydroxylterephthalate (HTA) were measured by photoluminescence spectroscopy every 30 min. Excitation was set to 315 nm and fluorescence intensities were measured at 425 nm.

Cell culture

HeLa cells were obtained from American Type Culture Collection (ATCC, Manassas, VA) and cultured in RPMI 1640 (GIBCO, Invitrogen) supplemented with heat-inactivated 10% FBS (fetal bovine serum, GIBCO, Invitrogen). HeLa cell lines were maintained in a humidified atmosphere of 5 % CO_2 at 37 ℃. Cells were cultured in 96 well plates at a density of 4×10^3 cells/well and were left for 24 h after treatment with melanin NPs solution (200 μL, various concentrations) as previously reported [28].

Cell viability assay (WST-1 Assay)

Cells were cultured in 96 well plates at a density of 4×10^3 cells/well and were left for 24 h after treatment with melanin NPs solution (200 μL, various concentrations). The supernatant of each well was then removed and washed twice with phosphate-buffered-saline (PBS), after which 10% WST-1 solution in media was added to each well followed by an additional 2 h of incubation at 37 ℃. 50 μL of supernatant from each well was then taken into a new plate to measure absorbance at 455 nm. The cell viability was determined relative to the absorbance of untreated control cells. Each experiment was performed four times to obtain average values.

Assays for effect of PMNPs on photo-sensitization of living cells

Cells were cultured in 96 well plates at a density of 4×10^3 cells/well and were left for 24 h after treatment with PMNPs solution (200 μL, 25 μg/mL).

The supernatant of each well was then removed and washed twice with PBS, after which each well was filled with 50 μL of PBS and exposed to hand-UV light (254 nm, 5 W) for 10 min. PBS was then replaced with the culture media, and after an additional 24 h of incubation, cell viability assays were performed.

To prepare samples for visual differentiation, HeLa cells at a density of 40×10^3 were cultured either with or without PMNPs (5 mL, 50 μg/mL), and were treated with trypan blue after washing and exposure to UV light.

2.3. Results and discussion

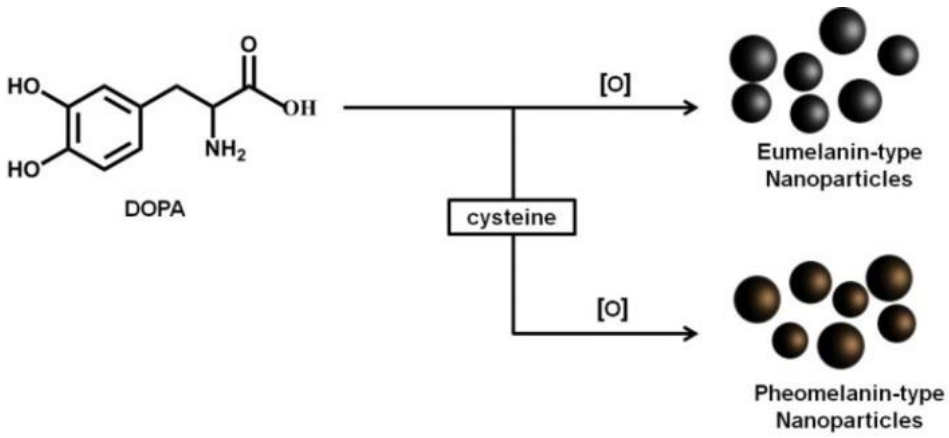

Scheme 2-1. Synthetic procedure for the preparation of eumelanin-type nanoparticles (EMNPs) and pheomelanin-type nanoparticles (PMNPs).

TEM images in Figure 2-1 show the morphology of prepared PMNPs and EMNPs, demonstrating that both have a similar spherical shape and size of approximately 100 nm. This suggests their suitability as models for naturally occurring melanins, as most natural melanins with living organisms demonstrate a comparable morphology [16, 17]. The size of PMNPs is slightly larger than the EMNPs probably due to the different kinetics and reaction mechanisms during the synthesis (Scheme 2-1). However, the size increase is not proportional to the amount of the incorporated cysteine (Figure 2-2).

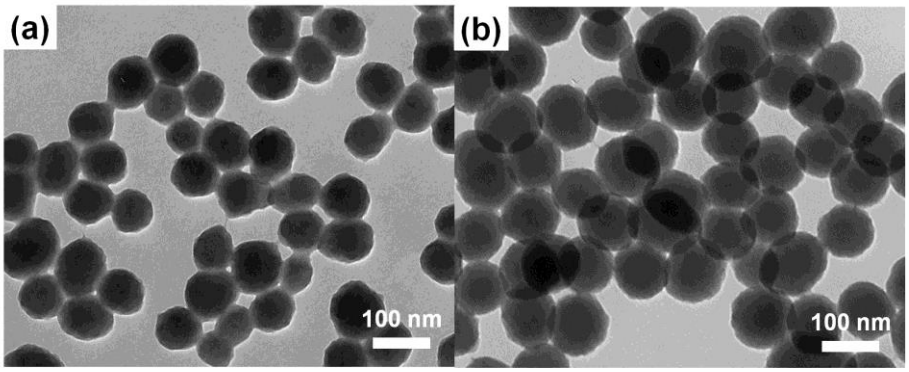

Figure 2-1. TEM images of (a) EMNPs and (b) PMNPs.

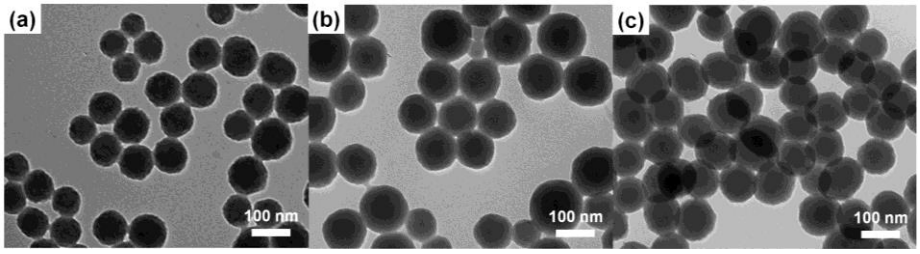

Figure 2-2. TEM images of PMNPs prepared at different ratios of DOPA to L-cysteine. (a) 1 : 0.5, (b) 1 : 1, and (c) 1 : 2.

cysteine/ DOPA	wt %				Empirical ratio		
	N	C	H	S	N	C	S
2	7.0155	37.4339	2.6978	2.4609	1	6.22	0.15
1	7.1131	36.4358	2.6026	2.1708	1	5.98	0.13
1/2	5.2806	28.0285	2.2808	0.7104	1	6.19	0.06
0	6.7188	39.5511	3.1055	·	1	6.87	0

Table 2-1. Elemental analysis (EA) of melanin NPs synthesized at various cysteine to DOPA ratios. Empirical ratio was calculated by dividing elemental percentage by atomic weight and normalizing to

nitrogen.

Elemental analysis (EA) data (Table 1) show additional differences, in this case with regards to chemical composition. As expected, sulfur was not detected in the EMNPs, while the relative ratio of sulfur in the PMNPs directly related to the amount of cysteine added, reaching a maximum in samples with an equivalent or great amount of cysteine added with regards to DOPA during synthesis. To ensure total conversion to PMNPs, all following samples were prepared using a cysteine/DOPA molar ratio of 2:1. PMNPs show a similar absorption to EMNPs in the UV-Vis region (Figure 2-3a). This broad and featureless absorption band is uncommon among organic chromophores and suggests that PMNPs contain a large number of energy states due to the heterogeneity of their chemical compositions [21]. Meanwhile, ESR data indicate the presence of stable free radical centers within the melanin nanoparticle structures, with the PMNPs data being distinct from that for the EMNPs (Figure 2-3b). This distinctive ESR signal with hyperfine splitting is associated with delocalization of an unpaired electron on the nitrogen of a semiquinoneimine moiety [22].

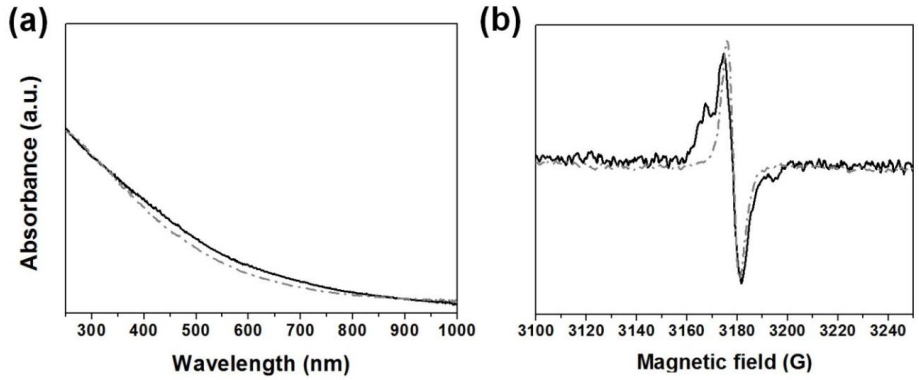

Figure 2-3. (a) UV-Vis absorption spectra and (b) ESR spectra of PMNPs (solid line) and EMNPs (dotted line).

Due to the characteristic features of melanins in biological functions, it is expected that heavy metals ions should be trapped on PMNPs during the synthesis. As expected, characteristic paramagnetic Mn^{2+} signals were clearly observed in ESR measurement as shown in figure 2-4. However, all the Mn^{2+} ions could be easily removed by washing with HCl solutions and ESR of washed samples confirmed the removal of Mn^{2+} by showing pheomelanin signals. Interestingly, the presence of Mn^{2+} ion showed no difference on the results of photo-sensitization effect of PMNPs.

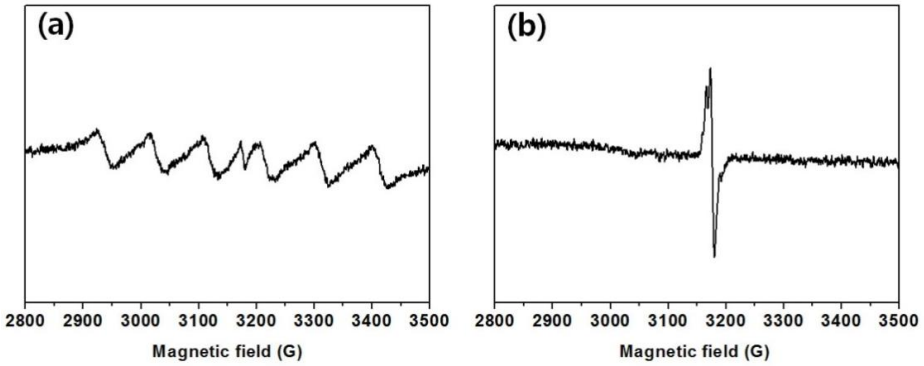

Figure 2-4. ESR spectra of PMNPs (a) before and (b) after removing Mn^{2+} ion with HCl solution.

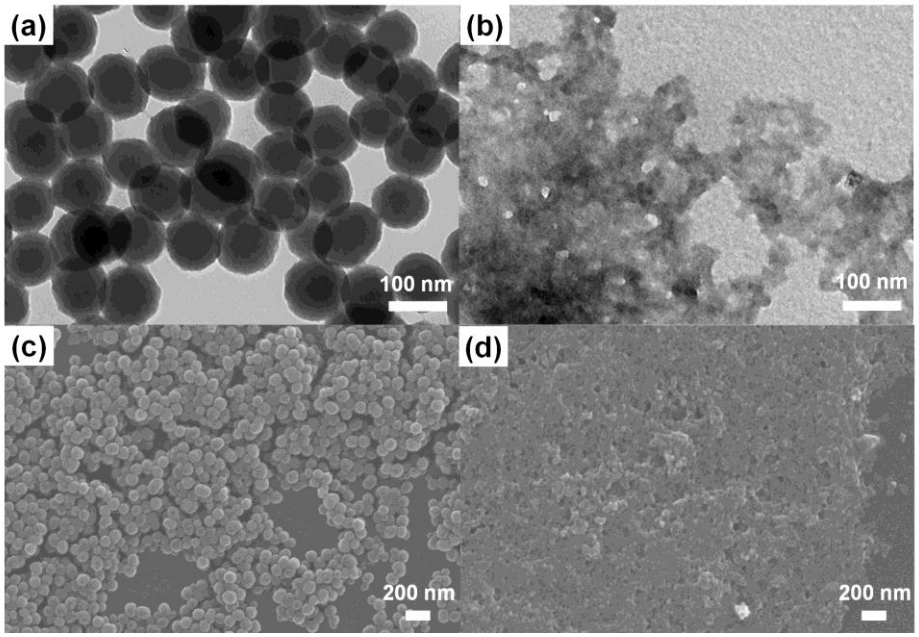

Figure 2-5. TEM images of (a) PMNPs and (b) Enzyme-pheoMels.

SEM images of (c) PMNPs and (d) Enzyme-pheoMels.

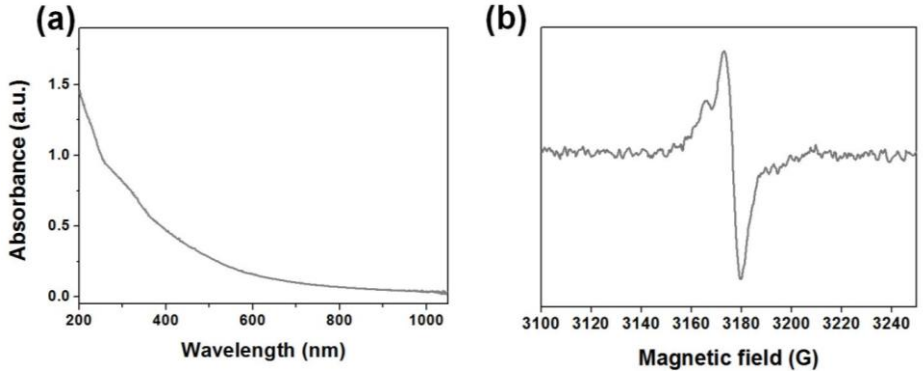

Figure 2-6. (a) UV-Vis absorption spectrum and (b) ESR spectrum of Enzyme-pheoMels.

Synthetic pheomelanin synthesized by tyrosinase (Enzyme-pheoMels) [23], which has been already proved to be very similar to natural pheomelanin [24], was used for comparison with the synthesized PMNPs. Although Enzyme-pheoMels (Enzyme-PMs) formed a cloudy mass that looked very different when compared to PMNPs (Figure2-5), the characteristic spectroscopic features (UV-Vis absorption and ESR spectra of Figure 2-6) and chemical analysis data (HPLC analysis result after HI reduction hydrolysis of Figure 2-7) proved to be very similar confirming that synthesized PMNPs have pheomelanin characteristics. Chemical analysis following well established methods by Ito group may prove of relevance that PMNPs are indeed pheomelanin and well comparison structurally with the so far reported synthetic pheomelanin as well as the spectroscopic features.

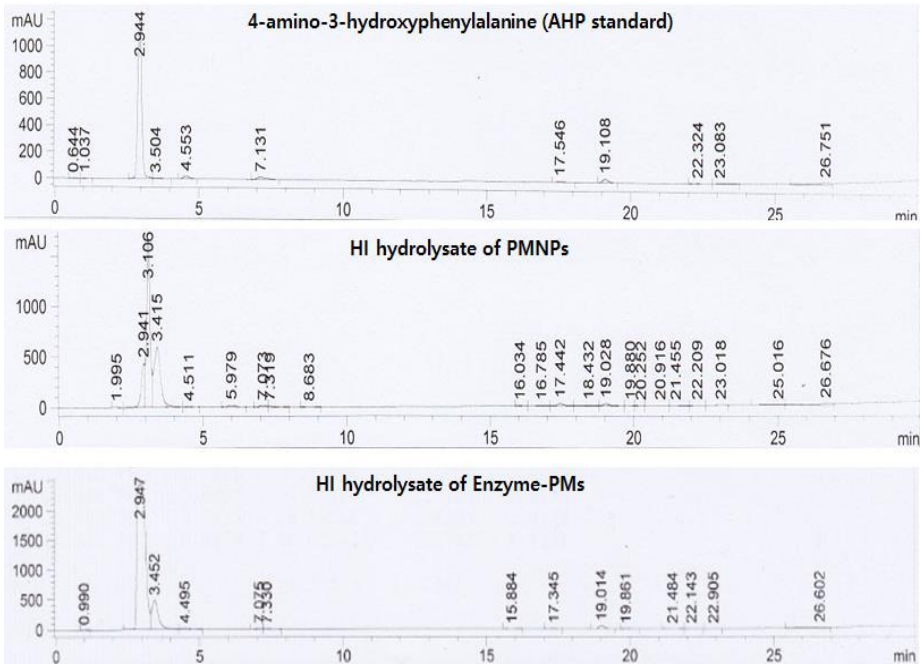

Figure 2-7. HPLC chromatograms detected in the positive mode of the each collect portion at the same retention time with the standard 4-amino-3-hydroxyphenylalanine (AHP) in HPLC from the reductive hydrolysis with hydriodic acid (HI); (a) PMNPs and (b) Enzyme-pheoMels. (modified from the reported method of K. Wakamatsu, S. Ito and J. L. Rees [24])

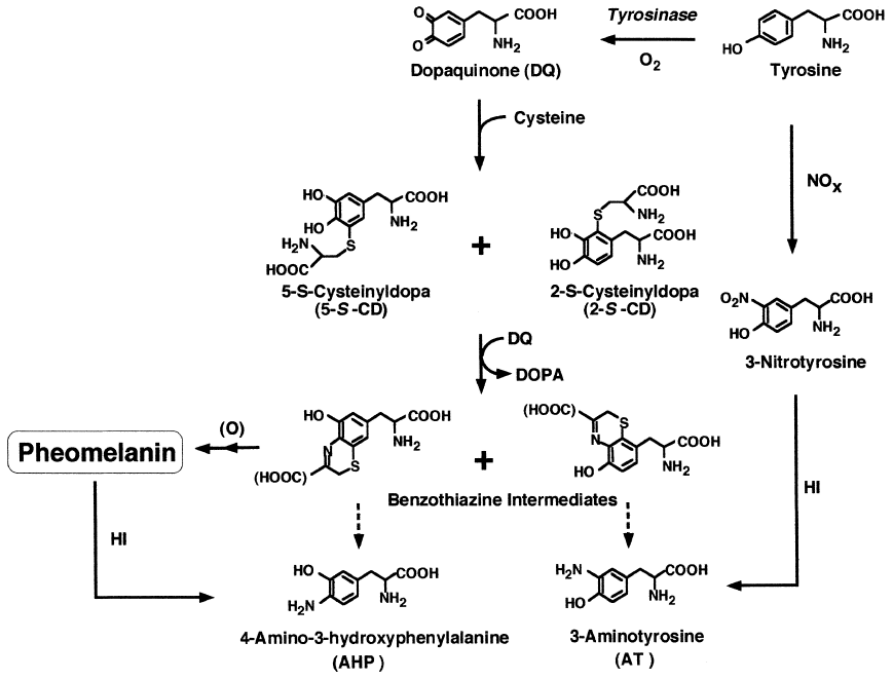

Scheme 2-2. Biosynthetic pathway to pheomelanin and the production of 4-amino-3-hydroxyphenylalanine (AHP) and 3-aminotyrosine (AT) from the benzothiazine units of pheomelanin, and the production of AT from 3-nitrotyrosine after HI reduction [24]

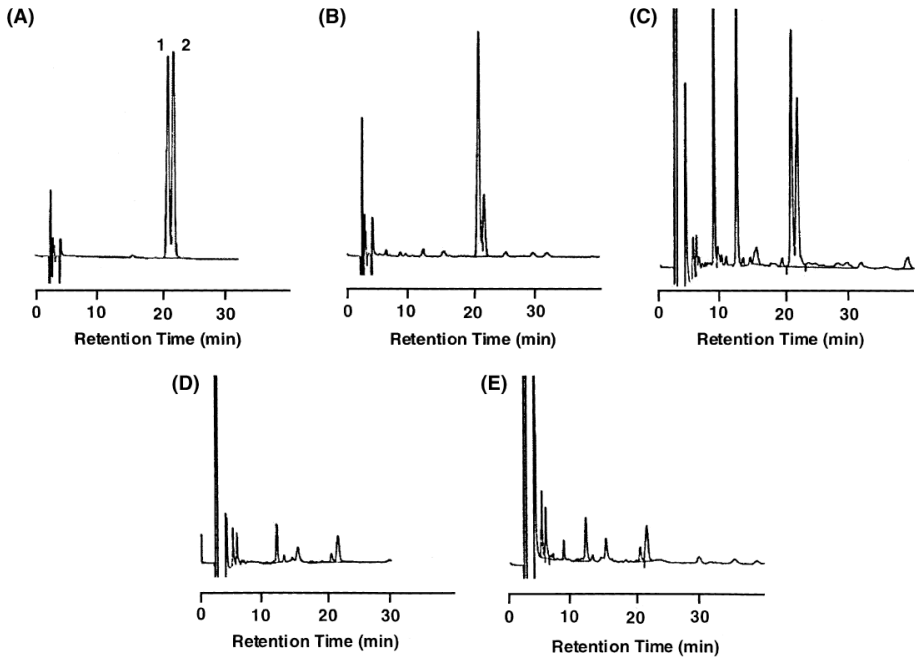

Figure 2-8. HPLC chromatograms of (A) specific AHP **(1**) and AT (**2**), (B) HI hydrolysate of synthetic pheomelanin (denoted as Enzyme-PMs), (C) HI hydrolysate of human red hair, (D) HI hydrolysate of human black hair, and (E) HI hydrolysate of human albino hair [24].

Even though these chemical analyses could not directly confirm the chemical structures of synthesized PMNPs, it was clearly shown that PMNPs have very similar hydrolyzed products such as AHP **(**4-amino-3-hydroxyphenylalanine, peak at RT=2.9) and AT (3-aminotyrosine, peak at RT=3.4). These hydrolyzed products were characterized as very specific maker molecules of pheomelanin both natural sources and enzyme-catalyzed synthetic one; which was clearly demonstrated in the reference 24 (Figure 2-8) that AHP and AT were only produced from pheomelanin sources and conclude that ‘specific

AHP' is a very specific marker of pheomelanin through the following suggested HI reduction hydrolysis mechanism (scheme 2-2). Therefore, we could conclude that PNMPs we prepared have similar chemical structures as natural pheomelanin which was already confirmed with enzyme-catalyzed synthetic pheomelanin along with other characteristic features of UV-Vis absorption and ESR measurements.

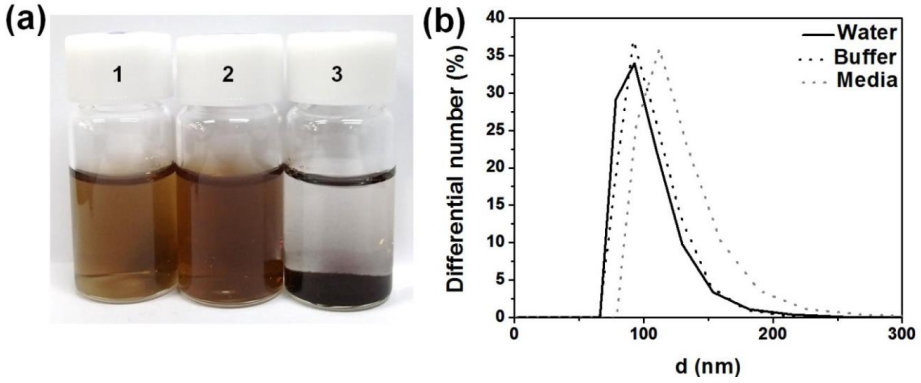

Figure 2-9. (a) Dispersion stability of (1) EMNPs, (2) PMNPs, and (3) Enzyme-PMs in neutral water, and (b) size distributions of PMNPs measured by Electrophoretic Light Scattering (ELS) method in water (solid line), PBS buffer solution (bold dotted line), and RPMI 1640 cell culture media containing FBS and PBS buffer solution (faint dotted line).

Electrophoretic Light Scattering (ELS) method was used to determine the long-term dispersion stability of PMNPs in various media, with results showing size distribution after storage for one day at room temperature in water, PBS buffer, and RPMI 1640 cell culture media (Figure 2-9). PMNPs

dispersed in cell culture media seem slightly bigger than those in other solutions; the possible interaction with proteins in the culture media might produce this result which is very similar to the surface adsorption of various materials on the surfaces of nanoparticles [25].

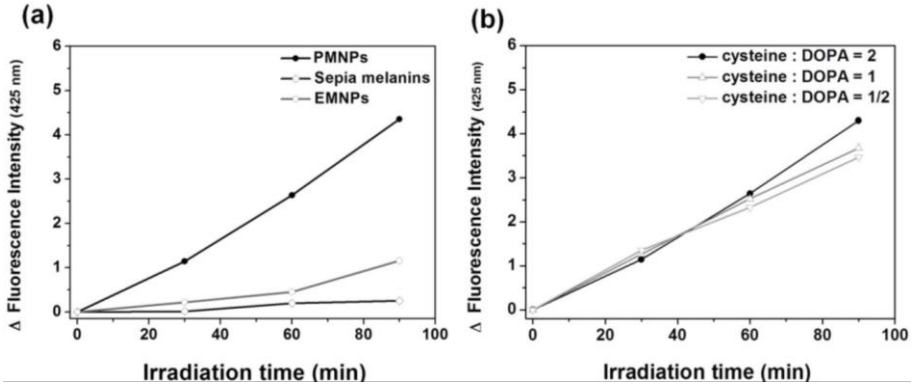

Figure 2-10. Generation of hydroxylterephthalate (HTA); (a) Time-profile of the fluorescence intensity at 425 nm from HTA photogenerated by 5 μg of PMNPs, EMNPs, and sepia melanin, and (b) time-profile of the fluorescence intensity at 425 nm from HTA photogenerated by various PMNPs prepared at varying ratios of cysteine to DOPA.

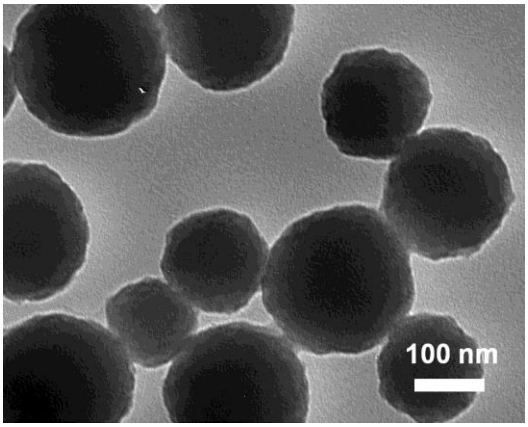

Figure 2-11. TEM image of purified sepia melanin nanoparticles.

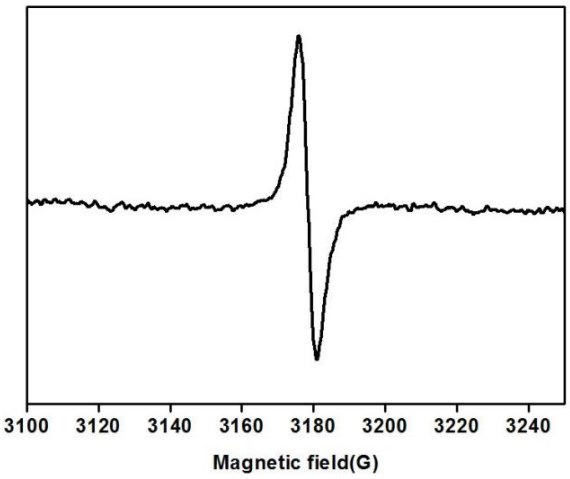

Figure 2-12. ESR spectrum of sepia melanin nanoparticles.

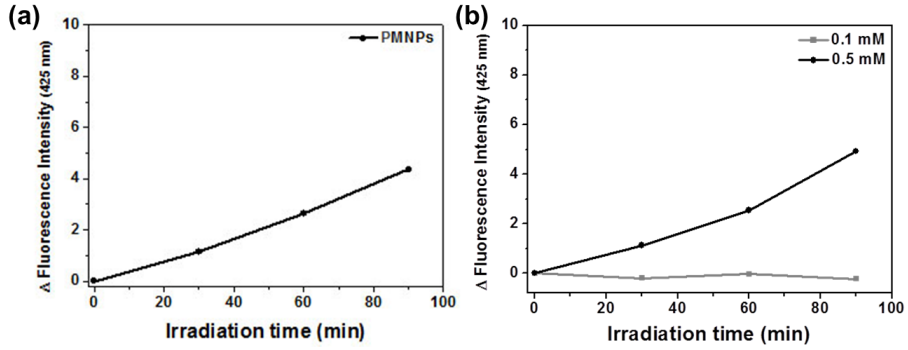

Figure 2-13. Time-profile of the fluorescence intensity at 425 nm from HTA; photogenerated by (a) 5 μg of PMNPs and (b) different amount of hydrogen peroxide.

Photophysical properties of the prepared water-dispersible PMNPs and EMNPs, as well as the purified sepia melanin (Figure 2-11, Figure 2-12), were investigated by monitoring the generation of hydroxyl radicals. Terephthalate (TA) was used as a probe molecule as it is known to generate fluorescent hydroxylterephthalate (HTA) through the interaction with hydroxyl radicals [26], which is considered as one of the major ROS through the complex processes of the O_2 sensitization by melanins [7-10].

HTA emits at 425 nm; the change in fluorescence intensity at this wavelength for PMNPs, EMNPs, and sepia melanins is shown in Figure 4a. PMNPs produced more hydroxyl radicals than the others; the amount produced by the natural sepia melanins is consistent with previously reported data [12,13], which is equivalent to the amount of H_2O_2 (~0.5 mM solution) by the generation of HTA (Figure 2-13).

However, PMNPs prepared by differing ratios of cysteine and DOPA did not show any significant difference in the generation of hydroxyl radicals (Figure 2-10b). More detailed investigation is needed to understand the effect of the amount of incorporated L-cysteine in the photo-sensitization of PMNPs; related studies are currently under way.

The effect of PMNPs photo-sensitization toward cancer cells was tested in-vitro by the cell staining method using trypan blue and the WST-1 cell viability assay. The cell staining method relied on confined exposure to determine the extent to which any cell death was the result of photosensitization (Figure 2-14).

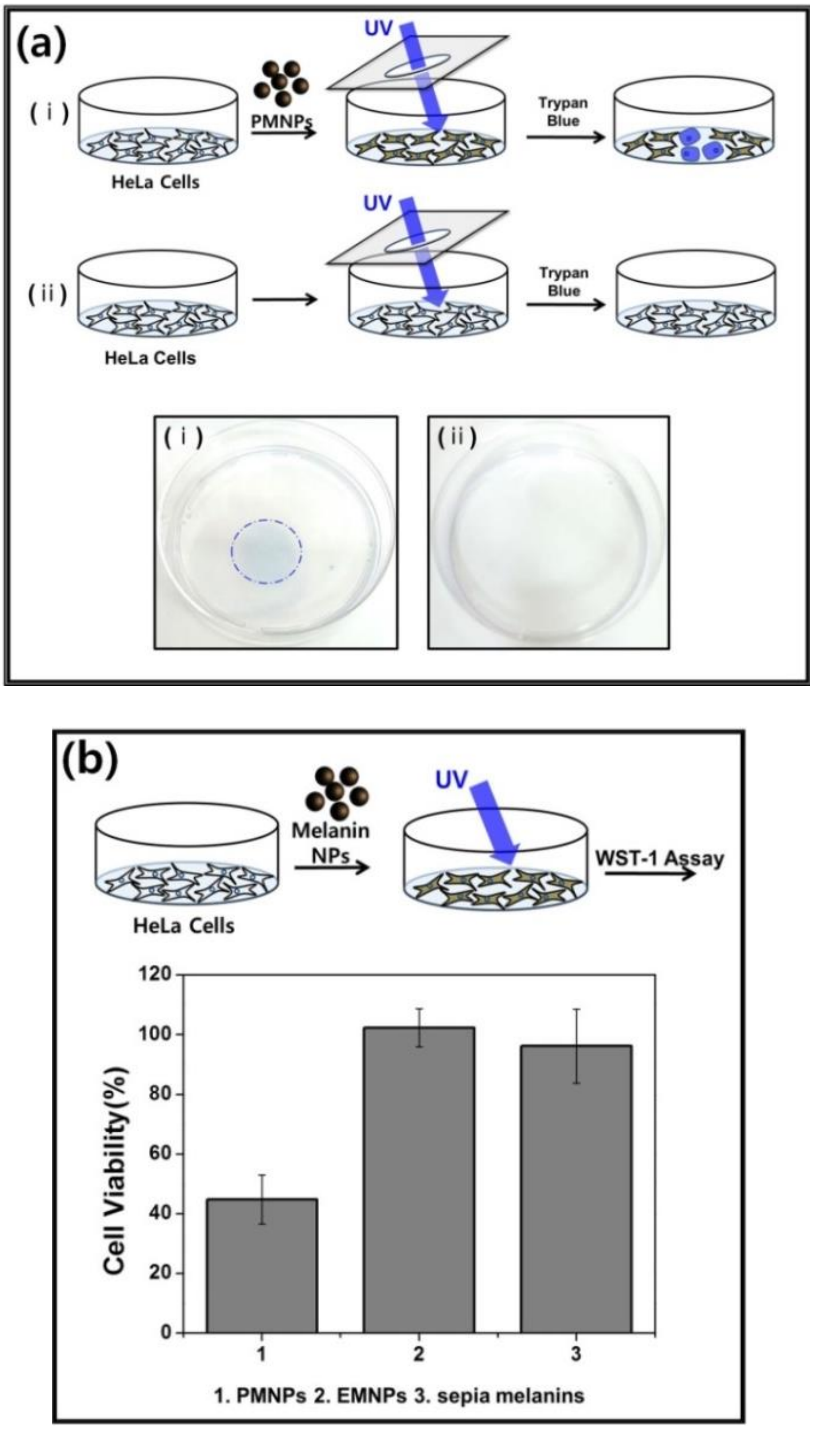

Figure 2-14. Photoinduced cytotoxicity of endocytosed melanin NPs in HeLa

cells; (a) trypan blue was applied to (i) HeLa cells containing PMNPs and (ii) particle-free HeLa cells after UV irradiation. (b) Viability test results of HeLa cells containing various melanin NPs after UV irradiation.

As expected, no staining was observed in cells treated with PMNPs but not exposed to UV light (outside of the dotted circle). HeLa cells not treated with PMNPs, on the other hand, did not show any staining differences even after UV irradiation (Figure 2-14a-ii). Endocytosis of PMNPs or irradiation in cells not treated with PMNPs did not show any staining differences even after UV irradiation. The need for both endocytosis of PMNPs and irradiation in eliciting cell death supports the conclusion that it resulted from photo-sensitization effect. It can be expected that the ROS generated outside of cells in the culture medium can affect the cytotoxicity results, even though the media were washed several times after the endocytosis of PMNPs. As shown below in the z-sectioned images of cells internalized with PMNPs (figure 2-15), no significant amount of particles were aggregated on the cell surfaces and most PMNPs seemed to be aggregated within the cell organelles most probably in the endosomes and lysosomes as previously reported for the internalization of nanoparticles into cells.

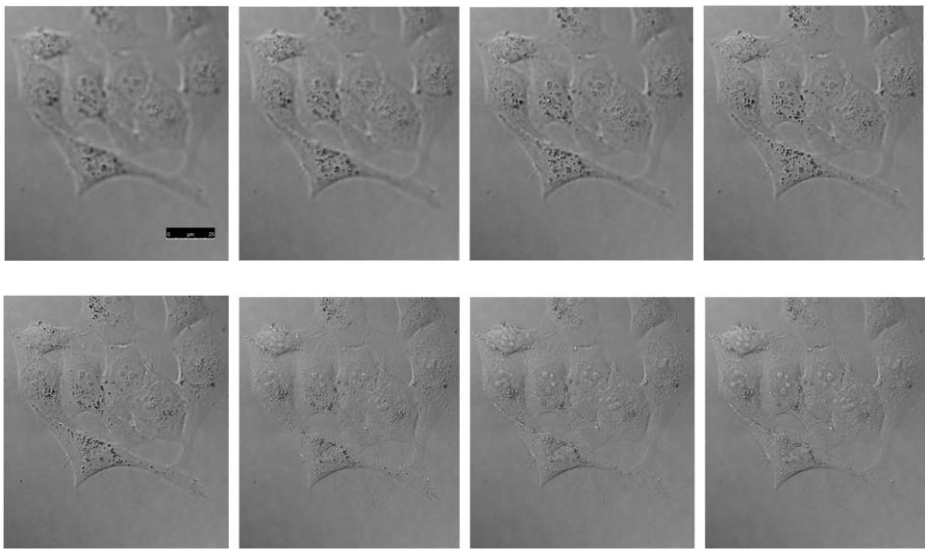

Figure 2-15. Z-sectioned images of cells internalized PMNPs. Focal depth was decreased from the bottom to the upper part of cells.

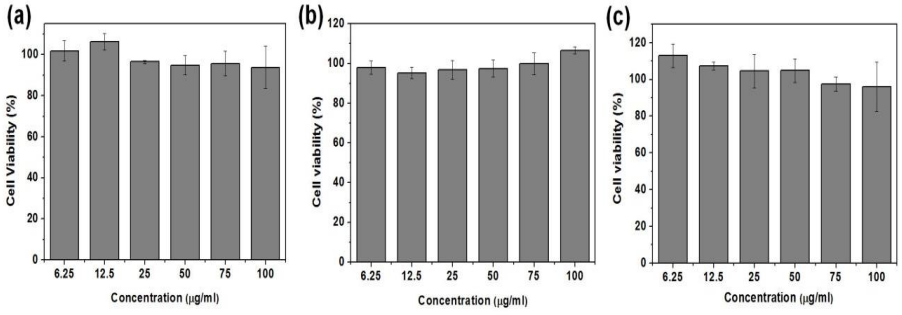

Figure 2-16. Result of WST-1 cell viability assay of HeLa cells with (a) sepia melanins, (b) EMNPs, (c) and PMNPs

Furthermore, HeLa cells treated with other melanin sources and exposed to UV light showed no significant color staining (results are not shown). These results were reinforced by the WST-1 assay (Figure 2-14b).

Cell viabilities presented are relative to the absorbance of particle-free and UV-irradiated control cells, and all treated nanoparticles exhibit no significant cytotoxicity up to a concentration of 100 μg/mL (Figure 2-16). PMNPs showed the highest phototoxicity (~50% viability) to HeLa cells under UV light when compared to EMNPs and sepia melanins, demonstrating a direct relationship to the relative efficiency of the hydroxyl radical generation (Figure 2-10a)

2.4. Conclusion

We successfully synthesized PMNPs from DOPA and cysteine by oxidative polymerization with $KMnO_4$. PMNPs exhibited a uniform size with a diameter of approximately 100 nm and an excellent dispersibility in both water and biological media. PMNPs were also biocompatible with cancer cells without showing any significant cytotoxicity up to a concentration of 100 μg/mL.

The photo-sensitization effects of PMNPs were systematically investigated by comparing them to those of EMNPs and natural sepia melanins. PMNPs produced more than four times the number of hydroxyl radicals when compared to the other melanins. PMNPs showed significant phototoxicity (~50% viability) to HeLa cells under UV light while EMNPs and sepia melanins did not show any toxicity effect, corroborating that phototoxicity was directly related to the generation of hydroxyl radicals. We believe that this simple method to synthesize water-dispersible PMNPs will aid melanin-related research in allowing for a greater understanding of the fundamental properties of natural melanins and, additionally, will make a significant contribution to particle-based nanotechnology by providing a new example of nontoxic and bio-inspired materials.

References

[1] J. D. Simon and D. N. Peles, The Red and the Black, Acc. Chem. Res. 43 (2010) 1452-1460.

[2] H. Z. Hill, The Function of Melanin or Six Blind People Examine an Elephant, Bioessays 14 (1992) 49-56.

[3] P. Meredith and T. Sarna, The physical and chemical properties of eumelanin, Pigm. Cell Res. 19 (2006) 572-594.

[4] S. Ito, K. Wakamatsu and H. Ozeki, Chemical Analysis of Melanins and its Application to the Study of the Regulation of Melanogenesis, Pigm. Cell Res. 13 (2000) 103-109.

[5] A. Thompson, E. J. Land, M. R. Chedekel, K. V. Subbarao and T. G. Truscott, A pulse radiolysis investigation of the oxidation of the melanin precursors 3,4-dihydroxyphenylalanine (dopa) and the cysteinyldopas, Biochim. Biophys. Acta 843 (1985) 49-57.

[6] S. Takeuchi, W. G. Zhang, K. Wakamatsu, S. Ito, V. J. Hearing, K. H. Kraemer and D. E. Brash, Melanin acts as a potent UVB photosensitizer to cause an atypical mode of cell death in murine skin, P. Natl. Acad. Sci. U.S.A. 101 (2004) 15076-15081.

[7] E. Wenczl, G. P. Van der Schans, L. Roza, R. M. Kolb, A. J. Timmerman, N. P. M. Smit, S. Pavel and A. A. Schothorst, (Pheo)Melanin Photosensitizes UVA-Induced DNA Damage in Cultured Human Melanocytes, J. Invest. Dermatol. 111 (1998) 678-682.

[8] I. A. Menon, S. Persad, N. S. Ranadive and H. F. Haberman, Effects of

Ultraviolet-visible Irradiation in the Presence of Melanin Isolated from Human Black or Red Hair upon Ehrlich Ascites Carcinoma Cells, Cancer Res. 43 (1983) 3165-3169.

[9] A. Hennessy, C. Oh, B. Diffey, K. Wakamatsu, S. Ito and J. Rees, Eumelanin and pheomelanin concentrations in human epidermis before and after UVB irradiation, Pigm. Cell Res. 18 (2005) 220-223.

[10] F. van Nieuwpoort, N. P. M. Smit, R. Kolb, H. van der Meulen, H. Koerten and S. Pavel, Tyrosine-Induced Melanogenesis Shows Differences in Morphologic and Melanogenic Preferences of Melanosomes from Light and Dark Skin Types, J. Invest. Dermatol. 122 (2004) 1251-1255.

[11] W. Korytowski, B. Pilas, T. Sarna and B. Kalyanaraman, PHOTOINDUCED GENERATION OF HYDROGEN PEROXIDE AND HYDROXYL RADICALS IN MELANINS, Photochem. Photobiol. 45 (1987) 185-190.

[12] L. J. Kirschenbaum, X. H. Qu and E. T. Borish, Oxygen radicals from photoirradiated human hair: An ESR and fluorescence study, J. Cosmet. Sci. 51 (2000) 169-182.

[13] X. H. Qu, L. J. Kirschenbaum and E. T. Borish, Hydroxyterephthalate as a Fluorescent Probe for Hydroxyl Radicals: Application to Hair Melanin, Photochem. Photobiol. 71 (2000) 307-313.

[14] Y. Liu, V. R. Kempf, J. B. Nofsinger, E. E. Weinert, M. Rudnicki, K. Wakamatsu, S. Ito and J. D. Simon, Comparison of the Structural and Physical Properties of Human Hair Eumelanin Following Enzymatic or

Acid/Base Extraction, Pigm. Cell Res. 16 (2003) 355-365.

[15] A. G. Bolt, INTERACTIONS BETWEEN HUMAN MELANOPROTEIN AND CHLORPROMAZINE DERIVATIVES Ⅰ, Life Sci. 6 (1967) 1277-1283.

[16] K. Jimbow, O. Ishida, S. Ito, Y. Hori, C. J. Witkop and R. A. King, Combined Chemical and Electron Microscopic Studies of Pheomelanosomes in Human Red Hair, J. Invest. Dermatol. 81 (1983) 506-511.

[17] T. Sarna, Properties and function of the ocular melanin- A photobiophysical view, J. Photochem. Photobiol. B 12 (1992) 215-258.

[18] Ozeki H, Ito S and Wakamatsu K. Chemical characterization of melanins in sheepwool and human hair. Pigm. Cell Res. 9 (1996) 51–57.

[19] Ozeki H, Ito S, Wakamatsu K and Hirobe T. Chemical characterization of hair melanins in various coat-color mutants of mice, J. Invest. Dermatol. 105 (1995) 361–366.

[20] D. J. Kim, K. Y. Ju and J. K. Lee, The Synthetic Melanin Nanoparticles Having An Excellent Binding Capacity of Heavy Metal Ions, B. Korean Chem. Soc. 33 (2012) 3788-3792.

[21] A. Huijser, A. Pezzella and V. Sundstrom, Functionality of epidermal melanin pigments: current knowledge on UV-dissipative mechanisms and research perspectives, Phys. Chem. Chem. Phys. 13 (2011) 9119-9127.

[22] R. C. Sealy, J. S. Hyde, C. C. Felix, I. A. Menon, G. Prota, H. M. Swartz, S. Persad and H. F. Haberman, Novel free radicals in synthetic and natural pheomelanins: Distinction between dopa melanins and cysteinyldopa

melanins by ESR spectroscopy, P. Natl. Acad. Sci. U.S.A. 79 (1982) 2885-2889.

[23] S. Ito, Optimization of Conditions for Preparing Synthetic Pheomelanin, Pigm. Cell Res. 2 (1989) 53–56.

[24] K. Wakamatsu, S. Ito and J. L. Rees, The Usefulness of 4-Amino-3-hydroxyphenylalanine as a Specific Marker of Pheomelanin, Pigm. Cell Res. 15 (2002) 225–232.

[25] M. Mahmoudi, I. Lynch, M. R. Ejtehadi, M. P. Monopoli, F. B. Bombelli and S. Laurent, Protein−nanoparticle interactions: opportunities and challenges, Chem. Rev. 111 (2011) 5610–5637.

[26] S. E. Page, W. A. Arnold and K. McNeill, Terephthalate as a probe for photochemically generated hydroxyl radical, J. Environ. Monitor. 12 (2010) 1658-1665.

[27] K. Y. Ju, Y. Lee, S. Lee, S. B. Park and J. K. Lee, Bioinspired Polymerization of Dopamine to Generate Melanin-Like Nanoparticles having an Excellent Free-Radical-Scavenging Property, Biomacromolecules 12 (2011) 625-632.

[28] K. Y. Ju, J. W. Lee, G. H. Im, S. Lee, J. Pyo, S. B. Park, J. H. Lee and J. K. Lee, Bio-Inspired, Melanin-like Nanoparticles as a Highly Efficient Contrast Agent for T_1-Weighted Magnetic Resonance Imaging, Biomacromolecules 14 (2013) 3491–3497.

Chapter 3

The effects of oxidation on melanins; alteration of physicochemical and photosensitizing properties

3.1 Abstract

Melanins protect tissue by absorption, non-radiative dissipation of ultraviolet light and interacts with reactive oxygen species with the persistent free radicals in their structure. However, melanins also produce reactive oxygen species (ROS) under UV radiation and are affected by oxidizing agent like ROS. Any chemical understanding of this ambivalent property of photoprotection and photosensitization of oxidized melanins has not been established. Herein, this issue is examined by studying hydrogen peroxide induced oxidation of melanins and ROS, especially singlet oxygen, generated by different oxidation states of melanins was directly measured. Oxidation of melanins results in structural disruption and has a significantly effects on the efficiency of singlet oxygen production.

3.2 Introduction

Natural melanins are important biological pigments with several well-established biological functions such as photoprotection, thermoregulation, metal chelator, free radical scavenger and photosensitization including skin pigment [1-3], yet they are still remained as poorly understood classes of biomacromolecules compared to other biomolecules such as proteins and nucleus. Researchers have intense characterized the molecular building blocks of melanins but overall architecture has not been able to described [4, 5].

Based on their intriguing physicochemical properties including their characteristic monotonic broadband absorption of UV light, extremely low radiative relaxation of photo-excited electronic states, the pigments have been thought to serve as an important role in photoprotective role and numerous protect-related researches of melanins have been carried out [6-8].

In direct contradiction with the photoprotective properties, melanins also show photosensitizing properties when UV light irradiation [9-11]. Negative implications to the photobiology of melanins such as cutaneous melanoma have also been reported. In vitro studies show that the UV light illumination of melanin generates reactive oxygen species and it is likely that under certain condition the excited species of melanins may provoke damaging instead of protecting process. This phenomenon in melanin can cause cell death through oxidative stress that implicates melanins photochemistry with destruction of DNA, suggesting a role of melanins in carcinogenesis although the underlying mechanism that the melanins act beneficial actions in the skin or takes part in

cell malignant transformation is not fully understood [12-15].

With regard to these ambivalent phenomena in melanins, the capacity of melanins to scavenge oxidizing species or how susceptible melanins are to degradative oxidation that may be induced by reactive oxygen species have been of broad interest to many researchers to understand the photophysical properties of melanins and the associated biological functions [16].

Oxidation of melanins has been an important chemical method for analysis of melanins and use of oxidizing agent such as hydrogen peroxide has aroused researchers' interest to understand the photophysical properties of melanins and the associated biological functions because hydrogen peroxide is related with the capacity of melanins to scavenge oxidizing species that may be induced by reactive oxygen species. Moreover, it affects the pigment's color, morphology and antioxidant behavior of melanins which might have important consequences for the biological functions that might related with the outbreaks of diseases. Moreover, the absorption of oxidized melanins significantly decreased in the red end of the spectrum, indicating such a change may affects the pigments' photoprotective function [17-19].

So far, however, the experimental approaches have been suffered from the lack of systematic of investigation of the photophysical properties following the oxidation of melanins. Since the difficulty in studying melanins itself, several melanin models have been proposed to understand its protective and photosensitizing properties associated with the oxidation of melanins. Only few researches show difference as the oxidation of melanins that cause

differences in its structure and therefore the associated photoreactivity of melanins [16, 20]. Furthermore, the consequent photosensitizing reactions of melanin with oxidation, especially singlet oxygen induced by the energy transfer from excited melanin to triplet oxygen, was never directly measured.

To study photophysical properties of melanin, especially their photosensitization, Melanin-like Nanoparticles (MelNps) were oxidized by hydrogen peroxide at neutral and low concentration of alkaline solution. MelNps are a synthetic melanin model which were successfully synthesized in our group before and are similar to the natural eumelanin in terms of photo-physical property, structural unit and morphological appearance [21]. Relatively strong oxidation with hydrogen peroxide in alkaline solution of MelNps accompanied structural disruption and we particularly called this alkaline hydrogen peroxide treated MelNps as melanin subunits.

Comparison of oxidized MelNps and bare MelNps is assessed by morphological change with TEM (transmission electron microscope) and for study of consequential difference in photophysical properties, the photooxidation of 1, 5-dihydroxynaphthalene (DHN) under visible light irradiation is adopted [22]. Moreover, the sensitive instrument based on the NIR phosphorescence emission of the singlet oxygen with a maximum at around 1270 nm was used to detect of generation of singlet oxygen directly.

3.3 Experimental Section

Chemicals and characterization

Dopamine hydrochloride, 1,3-dihydroxynaphthalene and the photosensitizer, meso-Tetraphenylporphine-4,4′,4″,4‴-tetrasulfonic acid tetrasodium salt (TSPP) were purchased from Sigma-Aldrich. Hydrogen peroxide solution and NaOH were purchased from Samchun. D_2O was purchased from Cambridge Isotope Laboratories, Inc. All of these chemicals were used without any further purification. The shape of the samples was determined by Transmission Electron Microscopy (TEM, Hitachi 7600) and UV-Vis spectra were recorded on a Hitachi, U-2900 spectrometry.

Preparation of melanin-like nanoparticles (MelNps)

We dissolved 180 mg of dopamine hydrochloride in 90 mL of the temperature stabilized deionized water at 50 ℃. Under vigorous stirring, 780 μL of 1 N NaOH solution was added to the dopamine hydrochloride solution. The color of solution changed yellow as soon as 1 N NaOH was added and gradually turned to dark black in an hour. The reaction was allowed to continue for an additional 4 h, after which melanin-like nanoparticles were collected by centrifugation (18,000 rpm, 15 min) and washed several times with deionized water. After large aggregated materials were removed by low speed centrifugation (4000 rpm), the final purified melanin-like nanoparticles were stored in deionized water [21].

Preparation of oxidized Melanin-like Nanoparticles (oxidized MelNps)

1 mg of MelNps were dispersed in 8.5 mL of deionized water. 1.5 mL of hydrogen peroxide solution was added to the solution and shaked to react for 3 h. The obtained oxidized MelNps were washed with deionized water twice through centrifugation (20000 rpm, 15 min) for remove any remaining peroxide in the solution and redispersed in 10 mL deionized water.

Preparation of melanin subunits

1 mg of MelNps was dispersed in 8.5 mL of 10 mM pH 10.5 phosphate buffer solution. 1.5 mL of hydrogen peroxide was added to the solution and the total volume of the solution was 10 mL. The color of the solution turned to pale yellow after 3h reaction which cannot collected any sedimentation by centrifugation at high speed.

Photooxidation experiments of 1, 5-dihydronaphthalene (DHN)

Photooxidation experiments of 1, 5-dihydroxynaphthalene by melanin samples were carried out in a quartz cuvette. An oxygen atmosphere was achieved by continuous bubbling of pure oxygen into the solution containing each melanin sample (MelNps, oxidized MelNps, subunit) and 1, 5-dihydroxynaphthalene (150 μM, 2 mL) while irradiation. For 10 μg of each

melanin sample, the concentration of 1, 5-dihydroxynaphthalene (DHN) in D_2O solution was 300 μM before addition of melanin samples (1 mL of 300 μM DHN solution, 100 μl of each 100 μL/mL melanin solution and 900 μL of D_2O solution). A 100 W Xenon lamp located at 10 cm from the cuvette which was filtered by a 410 nm filter to assure cut-off of the UV light. After given 5 min intervals of irradiation, the solutions in the cuvette were analyzed by UV-vis spectroscopy.

Singlet oxygen absorbance measurement

1 mg of MelNps and 1 mg of oxidized MelNps were dispersed in 10 mL D_2O after several centrifugation for exchange the solution for measurement. Subunits were freeze-dried since the product of treated alkaline hydrogen peroxide MelNps was not collected by centrigation. Freeze dried melanin sample was dispersed in D_2O right before the measurement. The Nd-YAG (Continuum surelite II-10, 10Hz, 7 ns FWHM pulse) pumped optical parametric oscillator (OPO) laser (Continuum OPO plus, 5 ns FWHM pulse) was used as an excitation source. Singlet oxygen phosphorescence signals were measured at perpendicular angle to excitation beam and detected through a monochromator (Optometrics LLC, mini-chrom04) and a NIR-PMT (Hamamatsu, H10330A). The signals were acquired by a 500 MHz digital oscilloscope (Agilent technology, DS07052A) and transferred to a computer for data analysis.

Singlet oxygen quenching measurement

Singlet oxygen was generated from photosensitizer, TSPP. 2 mL of 7 μM TSPP dispersed in D_2O was prepared for singlet oxygen quenching measurement. The excitation wavelength was 355 nm and the singlet oxygen NIR phosphorescence was detected at the wavelength of 1270 nm. 200 μL of melanin solutions were added to the TSPP solution to make solution concentration of 50 μg/mL, 100 μg/mL, 200 μg/mL and examine the change of singlet oxygen emission intensity generated from TSPP.

3.4 Result and discussion

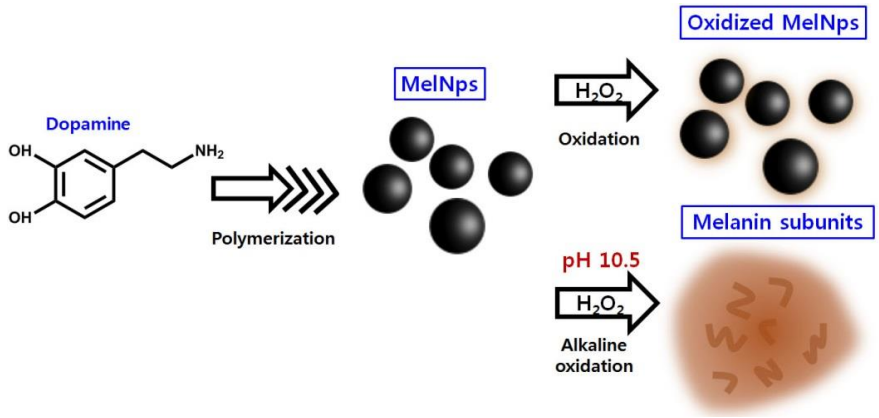

Scheme 3-1. Oxidation procedure of MelNps with hydrogen peroxide.

We synthesized MelNps, which had already been successfully synthesized in our group before, as a synthetic melanin model similar to the natural eumelanin in terms of photo-physical property, structural unit and morphological appearance. Moreover, MelNps have excellent water-dispersability without any additional chemical treatment [21]. As shown in scheme 1, oxidation of MelNps was performed by exposure to hydrogen peroxide and alkaline hydrogen peroxide. TEM images in figure 3-1 show the morphology and size of hydrogen peroxide treated and untreated MelNps. The MelNps obtained have uniform spheres, approximately 100 nm in diameter and no measurable change was seen in the particle size or morphology after treatment of hydrogen peroxide in neutral condition (see figure 3-1c, 3-1d), which make them facilitate the centrifugation to remove any residual

hydrogen peroxide in the solution. Oxidation in basic environment contributes hydrogen peroxide to activate its oxidizing power that morphological change of MelNps was observed (see figure 1e, 1f) [19]. We adapted respectively low concentration of buffer solution to make melanin subunits solution nearly neutral after 3 h reaction, followed by freeze drying process to remove remaining hydrogen peroxide. Although the low concentration of buffer solution, under the initially alkaline pH conditions, hydrogen peroxide is an efficient oxidant for melanins in contrast to the neutral pH condition and MelNps get out of their particle shape in 3 h and look amorphous which causes difficulty in procedure of centrifugation.

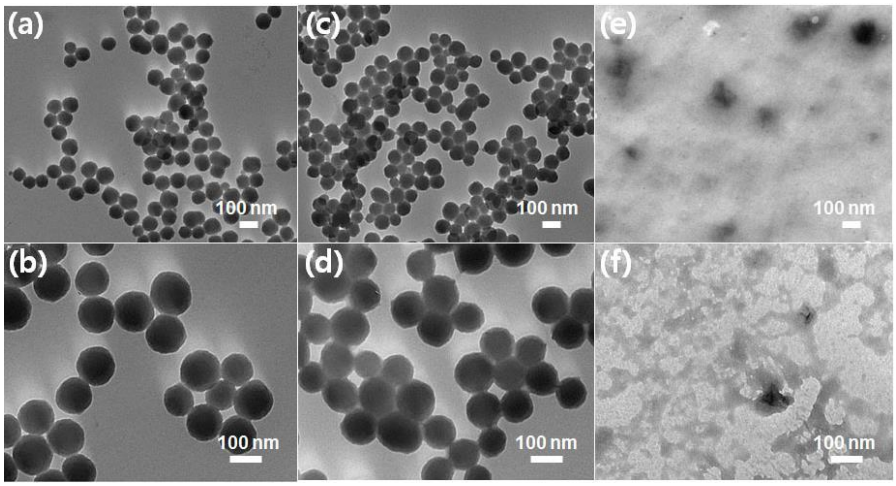

Figure 3-1. TEM images of (a),(b) MelNPs, (c),(d) oxidized MelNps (oxidized in neutral condition) and (e),(f) melanin subunits (oxidized in alkaline condition).

Absorbance spectra were measured by diluting to the same volume and mass concentration of each melanin solutions (Figure 3-2), even if their physicochemical properties might have some differences after exposure to oxidation conditions. The absorption spectra of MelNps decrease from the ultraviolet to the near infrared which is typically characteristic of the biological function of melanins in nature.

Absorption tendency of oxidized MelNps looks similar to that of MelNps except the slope of the graph in the region of short wavelength. Changes in absorption indicate that treatment of hydrogen peroxide causes the structural modification of MelNps and the increment in the region of short wavelength means some melanin fractions might exist with the oxidized MelNps solution even after purification which might affects their photophysical property. Melanin subunits show dramatically increment of short wavelength absorption, not extend over 600 nm. It matches with the TEM images of melanin subunits that there is no clear particle morphology found in Figure 3-1 (e) and 3-1 (f)).

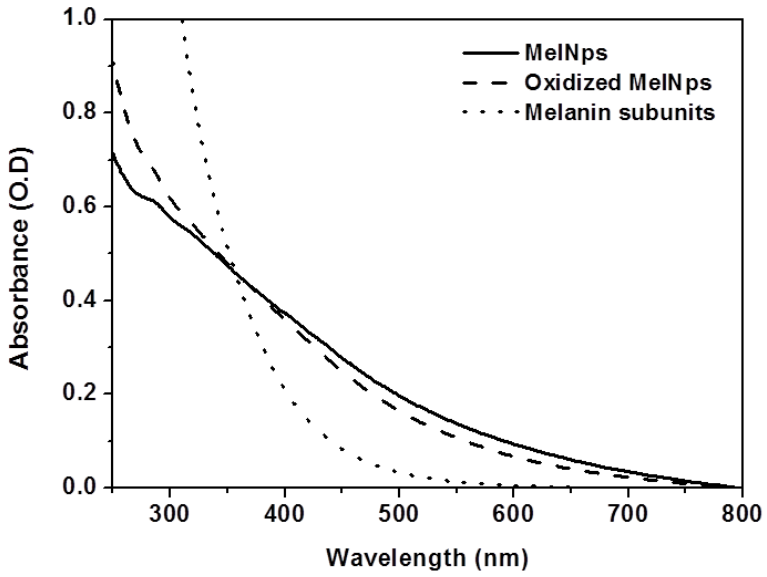

Figure 3-2. The absorption spectra of MelNps, oxidized MelNps and melanin subunits.

Difference in photophysical properties of melanins after oxidation with hydrogen peroxide was assessed by 1, 5-dihydroxynaphthalene (DHN). The DHN absorbance spectrum in water generally shows the band of 298 nm, 314 nm and 329 nm. Oxidation with singlet oxygen generated by oxidized MelNps under visible light irradiation in oxygen bubbling aqueous solution, DHN was oxidized to 5-hydroxyl-1, 4-naphtholquinone (juglone), which absorbs the light at 415 nm. The DHN absorbance spectrum in water generally shows the band of 298 nm 314 nm and 329 nm [22].

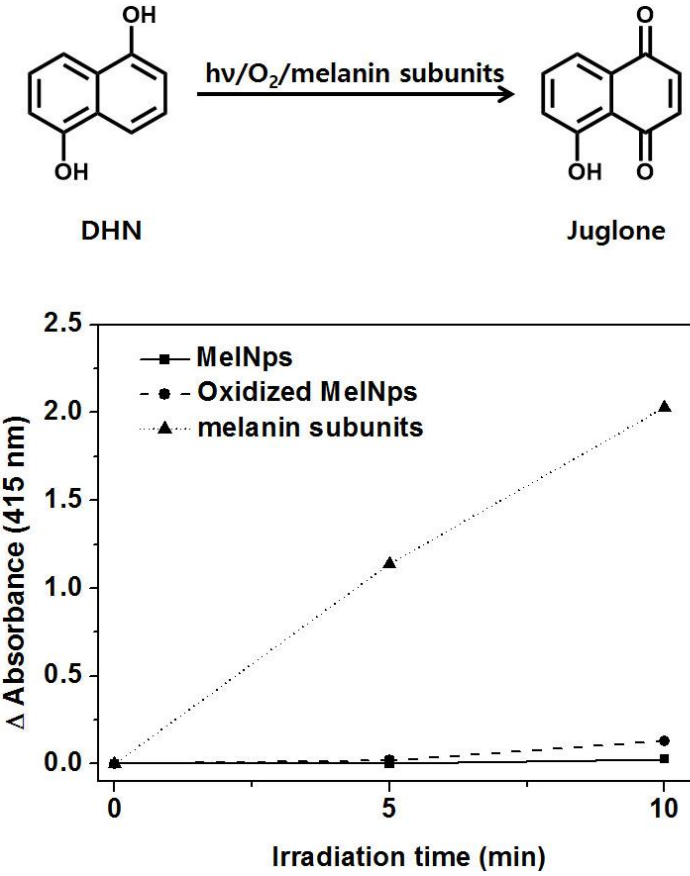

Figure 3-3. UV visible spectral changes at 415 nm of 1, 5-dihydroxynaphthalene (DHN) which are normalized by the optical absorption bands in the wavelength range 400-800 nm during photooxidation with 10 μg of (a) MelNps, (b) oxidized MelNps and (c) melanin subunits.

After irradiation, a noticeable new band was appeared in the visible region that is resulted from the oxidation of DHN with singlet oxygen that is produced by the melanins in the solutions. Considering that the absorbance of melanin subunits is concentrated in UV region (Figure 3-2), relatively small quantity of melanin subunits based on identical mass makes more singlet

oxygen than other melanins in this photooxidation of DHN since the irradiation wavelength is over the range of 400 nm. Normalization values by the same optical density in visible region of each melanin, melanin subunits shows great photosensitivity than other particle shaped melanins (Figure 3-3).

For the comparison, blank experiment irradiated only DHN solution also performed to check any difference in the absorbance bands after 10 min irradiation (Figure 3-4).

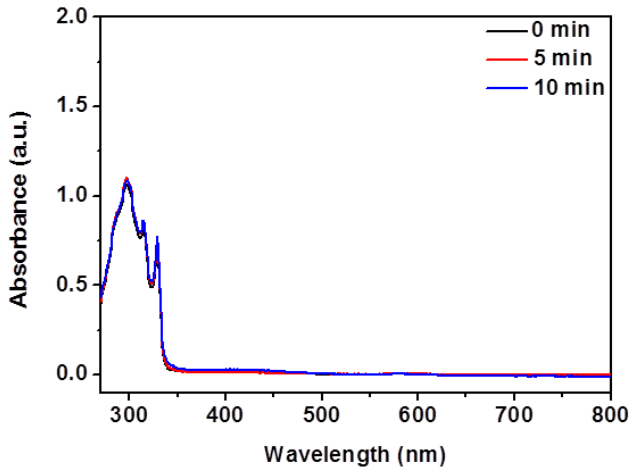

Figure 3-4. The absorption spectrum of 1, 5-dihydroxynaphthalene (DHN) solution without melanins.

The phosphorescence of singlet oxygen generated by oxidized MelNps under irradiation without any other photosensitizer was directly detected for the critical factor for the proof of singlet oxygen generation. Singlet oxygen detection was measured at the wavelength of 1270 nm which is the fingerprint

of the $O_2(a^1\Delta_g) \rightarrow O_2(X^3\Sigma_g^-)$ transition in D_2O solution [24]. The phosphorescence signals are shown in Figure 3-5. The decays are fitted to a single exponential function, resulting in the lifetime of the singlet oxygen that depends on the conditions. Measurements at excitation wavelength of 355 nm, identical optical density of each melanin, were performed to compare singlet oxygen generation capabilities of each melanin.

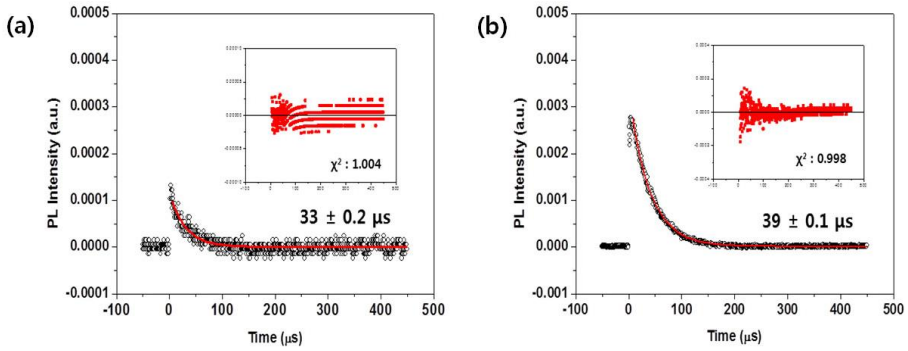

Figure 3-5. Phosphorescence decays of the singlet oxygen from (a) oxidized MelNps and (b) melanin subunits in D_2O at the detection wavelength of 1270 nm. There was no detective signal from MelNps. The solid lines are the fitted with a singlet exponential decay.

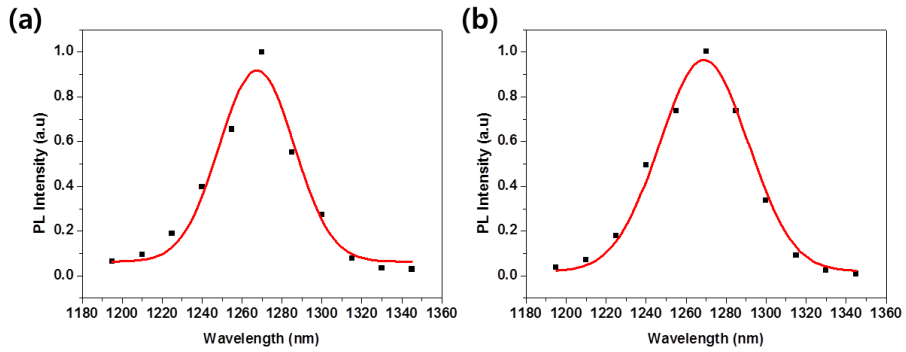

Figure 3-6. NIR phosphorescence emission spectra of (a) melanin subunits and (b) TSPP dispersed in D_2O.

Phosphorescence intensity of singlet oxygen generated from melanin subunits that were oxidized in activated hydrogen peroxide is higher than that of MelNps oxidized in neutral condition. There is no signal in MelNps solution and it is possible that the detection limit of spectroscopy might too low to detect the signal from the MelNps solution. The maximum emission was assessed and compared to the 5, 10, 15, 20-tetrakis (4-sulfonatophenyl) -porphyrin (TSPP) which was used as a standard photosensitizer (Figure 3-6).

Singlet oxygen quantum yield of oxidized MelNps and melanin subunits were calculated based on both identical optical density, using TSPP as a reference. Using the literature value of 0.67 for the quantum yield of reference compound [24], quantum yield for the production of singlet oxygen was obtained 0.0003 for oxidized MelNps and 0.009 for melanin subunits by the same photons absorbed at 355 nm. Melanin subunits generate approximately thirty times more singlet oxygen than oxidized MelNps which is consistent

with the result of experiment.

In addition to the intensity of the NIR spectral signal, the lifetime of singlet oxygen is another important parameter to be analyzed. The lifetime of singlet oxygen gives information of the environment of singlet oxygen that notifies the presence of physical or chemical quencher that causes a decrease in singlet oxygen lifetime. Typical lifetime of singlet oxygen reported is about 65 μs in D_2O. However, the singlet oxygen lifetime generated from melanins is shorter than the reported value [25, 26].

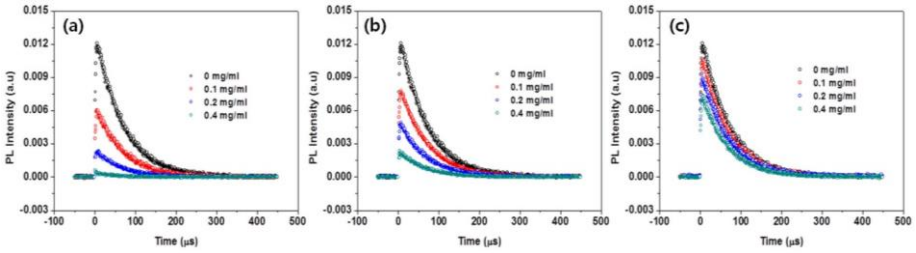

Figure 3-7. Singlet oxygen quenching efficiency of (a) MelNps, (b) oxidized MelNps and (c) melanin subunits. Singlet oxygen was generated by TSPP.

Sample		0 mg/ml	0.05 mg/ml	0.1 mg/ml	0.2 mg/ml
$^1O_2$ Lifetime	Melanin	67.2 ± 0.2 μs	66.5 ± 0.4 μs	61.8 ± 0.4 μs	46.5 ± 1.5 μs
	Oxidized melanin	67.6 ± 0.2 μs	67.8 ± 0.3 μs	64.5 ± 0.2 μs	62.0 ± 0.3 μs
	Melanin subunit	67.2 ± 0.2 μs	66.0 ± 0.2 μs	65.7 ± 0.3 μs	64.4 ± 0.2 μs

Table 3-1. Singlet oxygen lifetime of TSPP after treated with different amount of melanins.

Ambivalent characteristic of melanins, simultaneously possession of photoprotection and radical quenching properties, might contribute the shorten singlet oxygen lifetime. In this respect, radical scavenging experiment to check the ability to scavenge free radicals of melanins, especially singlet oxygen, was also performed. TSPP was used as a singlet oxygen generating agent to monitor the radical quenching properties of each melanin and melanin dependent changes in lifetime of singlet oxygen. Identical concentration of TSPP was used and the change of singlet oxygen intensity generated by TSPP with the different concentration of each melanin was measured in this quenching experiment. As shown in Figure 3-7, radical scavenging activity of melanin and oxidized melanins was investigated in dose dependent manner up to the concentration of 200 μg/mL. As increasing the amount of each melanin samples, singlet oxygen intensity from TSPP was decreased respectively and almost disappeared when 400 μg/mL MelNps was added to the TSPP solution, seemed MelNps to be a good singlet oxygen quencher. Moreover, singlet oxygen lifetime was affected considerably by the addition of MelNps (Table 3-1). While the melanin subunits, considering their own generation of singlet oxygen by themselves because they also activated under irradiation when 355 nm light (see Figure 3-5) used for activating TSPP, seemed to do little as a singlet oxygen quencher. As for the decrement of singlet oxygen lifetime generated from oxidized MelNps and melanin subunits themselves, it could be explained that the result of quenching

experiment shows that oxidized MelNps and melanin subunits can act as a quencher even though they are not as good as bare MelNps so that they might affect the singlet oxygen lifetime. In addition, the available site oxidized with hydrogen peroxide for generating or quenching activities of melanins is attributed to the degree of oxidation accompanied with their structural differences.

3.5 Conclusion

We have assessed oxidation-dependent photophysiscal properties of melanins through oxidation of the water dispersable MelNps similar to the natural melanins. Oxidation caused the absorption decrement in visible light, increment in UV region and change in their morphology especially oxidation of MelNps with alkaline hydrogen peroxide environment. The photooxidation of DHN with singlet oxygen generated by oxidized melanins and direct detection of the singlet oxygen suggest that oxidized melanins show significant photoreactivity. Oxidation of melanin also affects their photoreactivity as well as their efficiency of radical quenching property which is proved through the radical quenching experiment. In conclusion, the available site oxidized with peroxide for generating or quenching radical is interrelated with the degree of oxidation accompanied to the disassembly of structure and this is one of the crucial factors to opposite aspects of physicochemical properties and biological functions in bio-system. We believe that this approach to oxidation of melanins for understanding of physicochemical property serves a foundation for the understanding of the dichotomy of photoprotective and photoreactive properties of melanin associated with biological functions.

3.6 Reference

[1] G. Prota, Melanin and Melanogenesis, New York Academic Press (1992) 1–290.

[2] J. D. Simon and D. N. Peles, The red and the black, Acc. Chem. Res. 43 (2010) 1452–1460.

[3] H. Z. Hill, The Function of Melanin or Six Blind People Examine an Elephant, Bioessays 14 (1992) 49-56.

[4] P. Meredith, B. J. Powell, J. Riesz, S. P. Nighswander-Rempel, M. P. Pederson and E. G. Moore, Towards structure–property–function relationships for eumelanin. Soft Matter 2 (2006) 37–44.

[5] A. A. R. Watt, J. P. Bothma and P. Meredith, The supramolecular structure of melanin, Soft Matter 5 (2009) 3754-3760.

[6] J. Y. Lin and D. E. Fisher, Melanocyte biology and skin pigmentation, Nature 445 (2007) 843–850.

[7] P. Meredith and T. Sarna, The physical and chemical properties of eumelanin, Pigm. Cell Res. 19 (2006) 572-594.

[8] P. Meredith and J. Riesz, Radiative Relaxation Quantum Yields for Synthetic Eumelanin, Photochem. Photobiol. 79 (2004) 211-216.

[9] T. Sarna and R. C. Sealy, PHOTOINDUCED OXYGEN CONSUMPTION IN MELANIN SYSTEMS. ACTION SPECTRA AND QUANTUM YIELDS FOR EUMELANIN AND SYNTHETIC MELANIN, Photochem. Photobiol. 39 (1984) 69–74.

[10] I. A. Menon, S. Persad, N.S. Ranadive and H. F. Haberman, Formation of

superoxide and cell damage during UV-visible irradiation of melanin, Oxygen Radicals in Chemistry and Biology (Edited by W. Bors, M. Saran and D. Tait), Walter de Gruyter and Company, Berlin (1984) 673-679.

[11] T. Sarna and R. C. Sealy, PHOTOINDUCED OXYGEN CONSUMPTION IN MELANIN SYSTEMS. ACTION SPECTRA AND QUANTUM YIELDS FOR EUMELANIN AND SYNTHETIC MELANIN, Photochem. Photobiol. 39 (1984) 69–74.

[12] S. Takeuchi, W. G. Zhang, K. Wakamatsu, S. Ito, V. J. Hearing, K. H. Kraemer and D. E. Brash, Melanin acts as a potent UVB photosensitizer to cause an atypical mode of cell death in murine skin, P. Natl. Acad. Sci. U.S.A. 101 (2004) 15076-15081.

[13] A. Hennessy, C. Oh, B. Diffey, K. Wakamatsu, S. Ito and J. Rees, Eumelanin and pheomelanin concentrations in human epidermis before and after UVB irradiation, Pigm. Cell Res. 18 (2005) 220-223.

[14] M. R. Vincensi, M. d'lschia, A. Napolitano, E. M. Procaccini, G. Riccio, G. Monfrecola, P. santoianni and G. Prota, Phaeomelanin versus Eumelanin as a Chemical Indicator of Ultraviolet Sensitivity in Fair-skinned Subjects at High Risk for Melanoma: A Pilot Study, Melanoma Res. 8 (1998) 53–58.

[15] E. Wenczl, G. P. Van der Schans, L. Roza, R. M. Kolb, A. J. Timmerman, N. P. M. Smit, S. Pavel and A. A. Schothorst, (Pheo)Melanin Photosensitizes UVA-Induced DNA Damage in Cultured Human Melanocytes, J. Invest. Dermatol. 111 (1998) 678-682.

[16] J. M. Gallas, G. W. Zajac, T. Sarna and P.L. stotter, Structural

Differences in Unbleached and Mildly-Bleached Synthetic Tyrosine-Derived Melanins Identified by Scanning Probe Microscopies, Pigment Cell Res. 13 (2000) 99–108.

[17] S. Ito, Y. Nakanishi, R. K. Valenzuela, M. H. Brilliant, L. Kolbe and K. Wakamatsu, Usefulness of alkaline hydrogen peroxide oxidation to analyze eumelanin and pheomelanin in various tissue samples: application to chemical analysis of human hair melanins, Pigment Cell Melanoma Res. 24 (2011) 605–613.

[18] W. Korytowski and T. Sarna, Bleaching of melanin pigments. Role of copper ions and hydrogen peroxide in autooxidation and photooxidation of synthetic DOPA-melanins. J. Biol. Chem. 265 (1990) 12410–12416.

[19] Zareba M, Korytowski W, Sarna T, Truscott TG. The effect of degradation of neuromelanin on its free radical scavenging properties. Pigment Cell Res. 6 (1993) 300-347.

[20] Generation and suppression of singlet oxygen in hair by photosensitization of melanin Free Radical Biology & Medicine 51 (2011) 1195–1202.

[21] K. Y. Ju, Y. Lee, S. Lee, S. B. Park and J. K. Lee, Bioinspired Polymerization of Dopamine to Generate Melanin-Like Nanoparticles having an Excellent Free-Radical-Scavenging Property, Biomacromolecules 12 (2011) 625-632.

[22] J. H. Cai, J. W. Huang, P. Zhao, Y. J. Ye, H. C. Yu and L. N. Ji, Silica microspheres functionalized with porphyrin as a reusable and efficient

catalyst for the photooxidation of 1,5-dihydroxynaphthalene in aerated aqueous solution, Journal of Photochemistry and Photobiology A: Chemistry 207 (2009) 236–243.

[23] A. F. Uchoa, P. P. Knox, R. Turchielle, N. Seifullina and M. S. Baptista, Singlet oxygen generation in the reaction centers of Rhodobacter sphaeroides, Eur. Biophys. J. 37 (2008) 843–850.

[24] L. Shi, B. Hernandez and M. Selke, Singlet Oxygen Generation from Water-Soluble Quantum Dot-Organic Dye Nanocomposites, J. Am. Chem. Soc. 128 (2006) 6278-6279.

[25] C. Schweitzer and R. Schmidt, Physical Mechanisms of Generation and Deactivation of Singlet Oxygen, Chem. Rev. 103 (2003) 1685−1757.

[26] P. R. Ogilby, Singlet oxygen: there is indeed something new under the sun, Chem. Soc. Rev. 39 (2010) 3181–3209.

Appendix/Chapter 1

Disassembly of Melanin-like nanoparticles (MelNps) and their photo-physical property

1.1 Abstract

Melanins play as important role in photoprotection against UV-induced DNA damage by absorption of light and non-reactive dissipation of UV light. However, melanins also have photosensitizing property under UV irradiation. A chemical understanding of relationship between structure and biological function has not been established. Herein this issue is examined by disassembly of nanoaggregate state of eumelanin nanoparticle model to their subunit species under alkaline condition higher than pH 10.5 and comparison of photophysical properties of nanoggregated of eumelanin nanoparticle model with disassembled subunits. Disassembled subunits showed sharply increasing absorption in UV region and enhancement of emission as well as the photogeneration ability of reactive oxygen species which indicates of broad band absorbance of UV-vis light and non-reactive dissipation in nanoaggregated structure may be the key clue for understanding relationship between structure and biological functions of melanins.

1.2 Introduction

Eumelanins which make up most of the total melanin present in nature have been one of the most distinctive biomacromolecules because of their intriguing physicochemical properties. They have diverse biological functions like photoprotection, free radical quenching, photosensitization, metal ion chelation [1-3]. Based on their physicochemical properties including broadband absorbance of UV-visible light with non-radiative relaxation, they have been suggested to play an important role in photoprotection in bio-system [4, 5]. However, not only their beneficial biological functions but also some implications in correlation with risk factors of disease such as skin cancer and neurodegenerative disorder like Parkinson's disease make eumelanin challenging biomaterial. In this regard establishment of relationship between structure and biological function of melanin has been one of the main issues for understanding various biological behaviors of eumelanins [6-9].

However, the precise molecular structure of eumelanins has remained elusive. Even though researchers have characterized the molecular building blocks of eumelanins which has been general agreement with the composition of 5, 6-dihydroxyindole (DHI) and 5, 6-dihydroxyindole-2-carboxylic acid (DHICA), there is no accepted definite secondary structure [10, 11]. Lately, nanoaggregates of stacked oligomeric unit modes have been proposed which is more close to nature of the macromolecular structure of eumelanins but overall architecture of the pigments still has not been able to describe [12, 13].

Unfortunately, there are some limitations for studying of structure-property-biological function relationship of eumelanins. Most of the synthetic eumelanin models cannot be generated as three dimensionally aggregated particles with nano-sized scale like natural eumelanins. Moreover, there is no standardized procedure to extract from natural sources with maintenance of their intact structural and physicochemical properties [14-16]. Insolubility of most eumelanin models is another difficulty in melanin study because alkaline solutions are generally used for solubilization of eumelanin which is not exactly understood of the effect on the physicochemical properties and structure of eumelanin before characterization [17].

In this chapter, we demonstrate disassembly of eumelanin nanoparticles to their subunit species under alkaline condition higher than pH 10.5. Melanin-like nanoparticles (MelNps) was used as a synthetic eumelanin model which were successfully synthesized in our group before and are similar to the natural eumelanin in terms of photo-physical property, structural unit and morphological appearance [18]. We further investigated nanoaggregate structure-photophysical function relationship by comparison of photophysical properties of nanoggregated of eumelanin model, MelNps, to that of disassembled subunits.

1.3 Experimental section

Preparation of melanin-like nanoparticles (MelNps)

We dissolved 180 mg of dopamine hydrochloride (Aldrich Chemical) in 90 ml of the temperature stabilized deionized water at 50 ℃. Under vigorous stirring, 780 μL of 1 N NaOH solution was added to the dopamine hydrochloride solution. The color of solution changed yellow as soon as 1 N NaOH was added and gradually turned to dark black in an hour. The reaction was allowed to continue for an additional 4 h, after which melanin-like nanoparticles were collected by centrifugation (18,000 rpm, 15 min) and washed several times with deionized water. After large aggregated materials were removed by low speed centrifugation (4000 rpm), the final purified melanin-like nanoparticles were stored in deionized water.

Disassembly of eumelanin model in basic solution

20 mg of MelNps was dispersed in 16 ml deionized water and 4 mL of 1 M NaOH solution was added into the MelNps to make total volume of solution 20 ml (1 mg/mL, 0.2 M NaOH). 500 μl of solution were collected every day and disassembled subunits were obtained by 14500 rpm of centrifugation for 10 min to separate from particles. PL spectra of supernatant were measured for kinetic study of disassembled subunits during disassembly process. After 4 days, completely disassembled subunits are obtained. PL spectra and UV-Vis absorption spectra were recorded on a JASCO and SINCO S-3100

spectrometer.

Photogeneration of hydroxyl radical by MelNps and disassembled melanin subunits

The solutions of dispersed MelNps (100 μg/mL, 50 μL) and disassembled subunits were mixed with deionized water (1.55 mL) in a quartz cuvette. Freshly prepared TA solution (400 μL, 20 mM) was then added to the solution, and the cuvette was capped to prevent solvent loss. The sample was then irradiated by a xenon lamp at a distance of 10 cm for a total of 1 h. Fluorescence intensities from the generated hydroxylterephthalate (HTA) were measured by photoluminescence spectroscopy. Excitation was set to 315 nm and fluorescence intensities were measured at 425 nm. Fluorescence was recorded on JASCO.

Photogeneration of superoxide by MelNps and disassembled melanin subunits

The solutions of dispersed MelNps (100 μg/mL, 50 μL) were mixed with 1 M phosphate buffer (1.55 mL) in a quartz cuvette. Freshly prepared NBT (nitro blue tetrazolium chloride) solution (400 μL, 0.2 mM) was then added to the solution, and the cuvette was capped to prevent solvent loss. The sample was then irradiated by a xenon lamp at a distance of 10 cm for a total of 1 h. The reduction of NBT was followed at 560 nm in terms of the production of formazan, which exhibits a broad absorption maximum in this region of the

spectrum. UV-vis spectra were recorded on SINCO-3100 apparatus.

1.4 Result and discussion

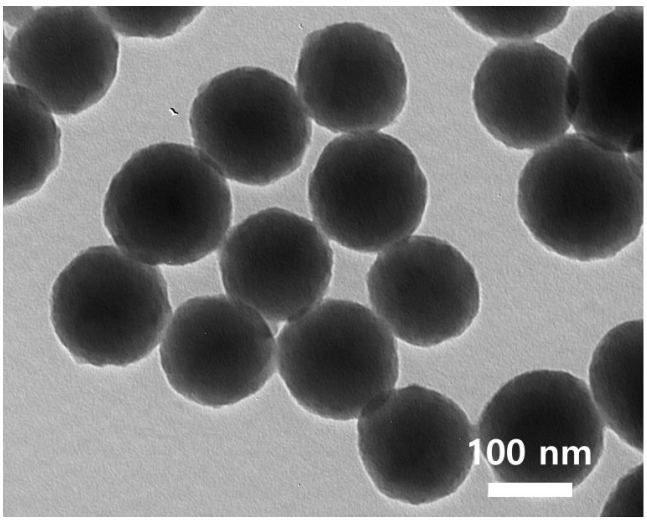

Figure 1-1.TEM image of melanin-like nanoparticles (MelNps).

Melanin-like Nanoparticles (MelNps), which had already been successfully synthesized in our group before, as a synthetic eumelanin model similar to the natural eumelanin in terms of photo-physical property, structural unit and morphological appearance, were synthesized for the examination in disassembly of nanoaggregate of eumelanin. Synthesized by spontaneous oxidation of dopamine, MelNps is an appropriate model for examination of disassembly nanoaggregated nanostructure eumelanin because polydopamine synthesized by autooxidation of dopamine has been illustrated as supramolecular aggregates of monomers similar to the structure of eumelanin

[19-22]. MelNps have also great water dispersibility without any additional chemical treatment and transmission electron microscopy (TEM) image in Figure 1-1 shows the size and morphology of MelNps.

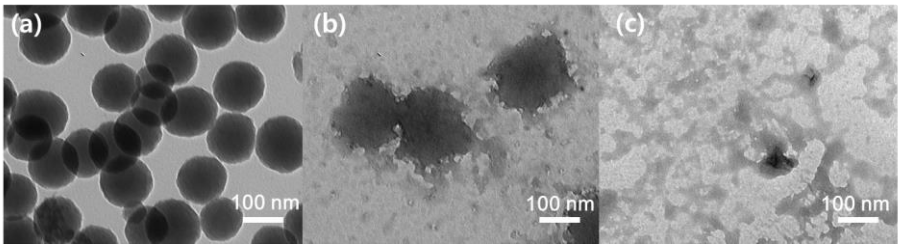

Figure 1-2.TEM images of MelNps before (a) and after (b) exposure in basic solution for a day and (c) for 4 days.

Disassembly of MelNps was induced by directly exposure in basic solution (pH 10.5) and morphological change was in MelNps observed by TEM (Figure 1-2). After exposure of MelNps in alkaline environment for a day, they showed coexistence with disassembled subunits, particles and some aggregates that precipitate by centrifugation but lost particulate nature. For 4 days exposure in basic solution, only disassembled subunits are left in the solution with amorphous shape.

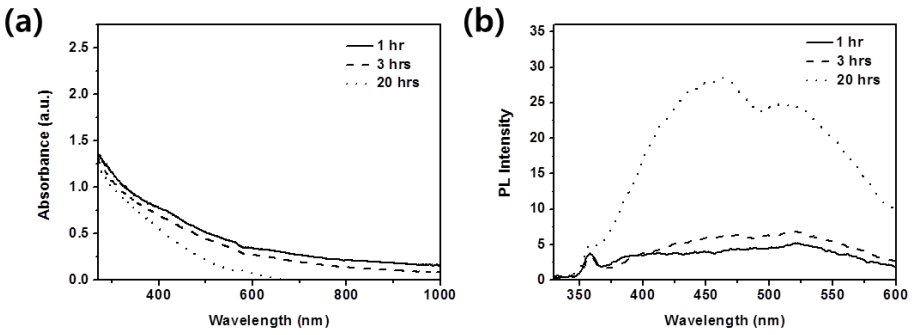

Figure 1-3. (a) UV-vis spectra and (b) PL intensity of disassembled subunits in supernatant solution after centrifugation of basic solution (λ_{ex} = 320 nm).

Disassembly of MelNps caused their broad band absorption of UV-vis. Figure 1-3 shows the absorbance change of disassembled subunits in the supernatant separated during the disassembly process in basic solution followed by centrifugation process. Long exposure time in basic solution leads the optical density decrement of visible region and increment in UV region and this is well consistence with degree of morphological change. 1 h and 3 h exposure samples have still aggregates with subunits in supernatant that precipitate after centrifugation.

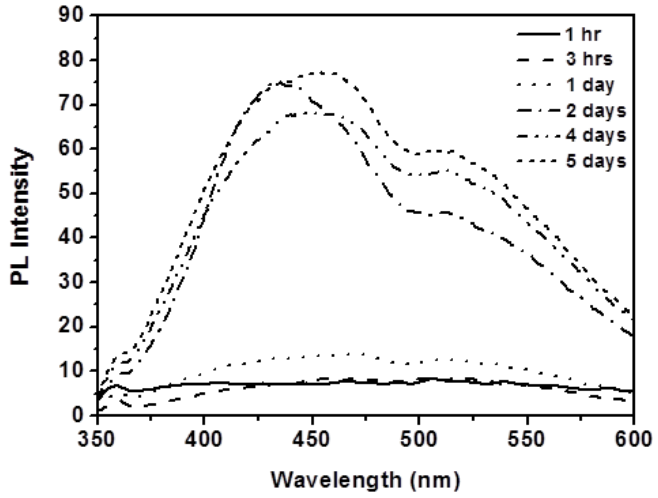

Figure 1-4. Enhancement in fluorescence emission of .disassembled MelNps during assembly process

Fluorescence emission with extremely low radiative quantum yield of light is one of the important photophysical properties related with the photoprotective function of eumelanin. However, in contrast of the low fluorescence of nanoaggregate MelNps, disassembled subunits in the supernatant increased during the disassembly process that indicates aggregation structure of MelNps is attributed to light dissipation property related with photoprotection of eumelanin [23-25]. It seems that almost all of the MelNps are disassembled after 4 day because there is no increment of fluorescence intensity (Figure 1-4).

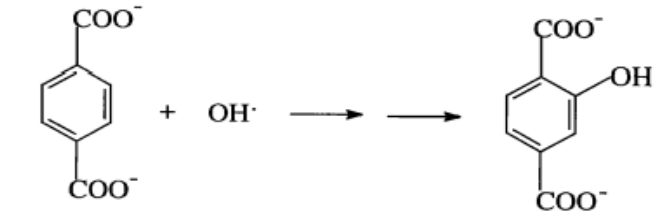

Terephthalate (TA) (Non-fluorescent)

2-hydroxyterephthalate (HTA) (Fluorescent: λ_{ex} = 315 nm, λ_{em} = 425 nm)

Figure 1-5. Terephthalic acid (TA) used to measure sonochemically produced hydroxyl radical production via the fluorescence spectrum of the hydroxyl adduct [26]

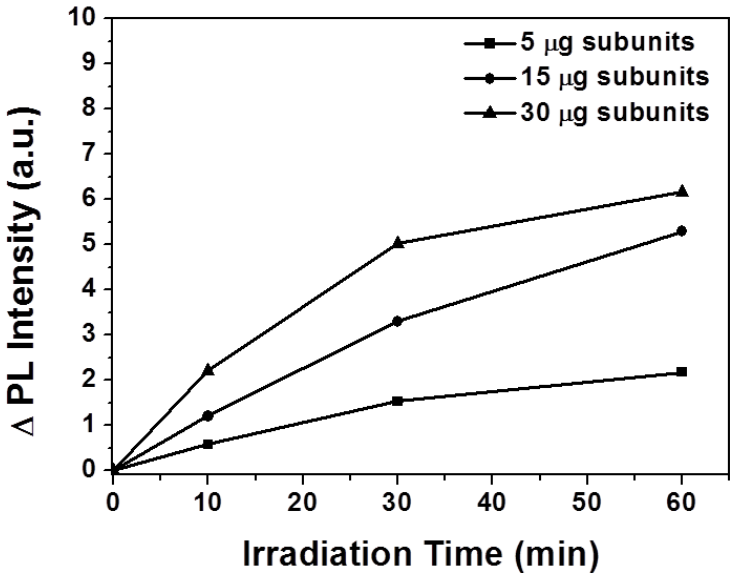

Figure 1-6. Time profile of enhancement in fluorescence of 2-hydroxyterephthalate (HTA) by disassembled subunits.

Photogeneration capability of reactive oxygen species (ROS) by disassembled subunits were examined with terephthalate (TA) which is one of the fluorescence probe detect hydroxyl radical through fluorescence of hydroxyl radical adduct, 2-hydroxyterephthalate (HTA) at 425 nm. HTA emission intensity increased in proportion to concentration of subunits which were fully disassembled for 4 days (Figure 1-6). However, there was no significant fluorescence increment in MelNps during irradiation compared to that of subunits which indicates that MelNps cannot produce hydroxyl radical effectively

.

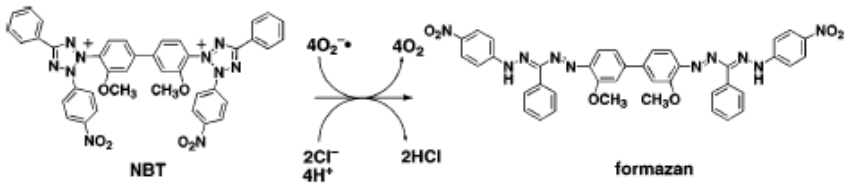

Figure 1-7. The reduction of NBT (nitro blue tetrazolium) by superoxide to produce of formazan which exhibits a broad absorption maximum in this region of 560 nm.

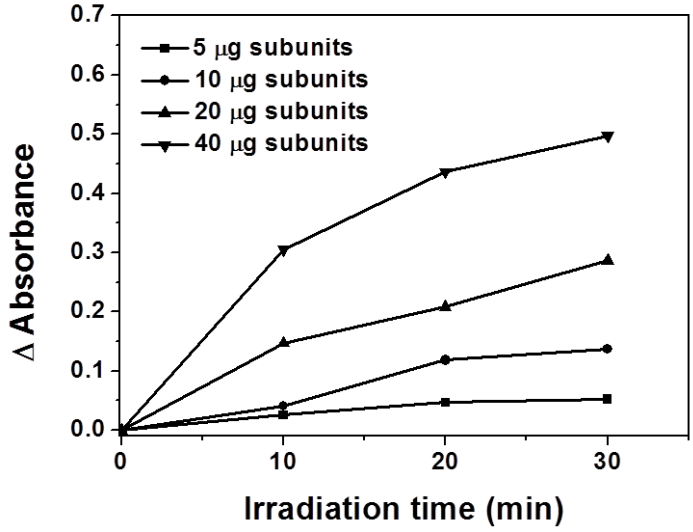

Figure 1-8. Time profile of enhancement in absorption of formazan by disassembled subunits at the wavelength of 560 nm.

In addition, NBT (nitro blue tetrazolium) was used for detection of superoxide generated by disassembled subunits. . Due to the pH of disassembled subunits in basic solution is high, aliquot of disassembled subunits in basic solution was transferred to the pH 7.4 buffer solution containing NBT. NBT is reduced by superoxide to make formazan which has absorption maximum at 560 nm and absorption of solutions with disassembled subunits increased in proportion to concentration of disassembled subunits as the irradiation time increases during irradiation [27]. MelNps have no absorbance change in the wavelength of 560 nm in contrast to the disassembled subunits similar in the hydroxyl radical assay used TA.

Different efficiency of photogeneration for hydroxyl radicals and superoxide

of MelNps and their disassembled subunits demonstrates that photoprotective function of nanoaggregated MelNps turns to photoreactive function when they lose their nanoaggregate structural character.

1.5 Conclusion

We examined disassembly of nanoaggregated eumelanin nanoparticle model in basic condition which is accompanied with change in their photophysical property. Disassembled subunits showed sharply increasing absorption in UV region and enhancement of emission.

In addition, disassembly cause generation of reactive oxygen species like superoxide and hydroxyl radical which is the opposite aspect of melanin in terms of photoprotective function in biological system. As a result, photophysical property of broad band absorbance of UV-vis light and non-reactive dissipation of melanins is closely correlated to the nanoaggregated structure and this is the crucial factor of understanding diverse and opposite properties of melanins.

1.6 Reference

[1] G. Prota, Melanins and Melanogenesis, Academic Press 1992.

[2] J. D. Simon and D. N. Peles, The Red and the Black, Acc. Chem. Res. 43 (2010) 1452-1460.

[3] L. Hong and J. D. Simon, Current Understanding of the Binding Sites, Capacity, Affinity, and Biological Significanceof Metals in Melanin, J. Phys. Chem. B 111 (2007) 7938-7947.

[4] P. Meredith and J. Riesz, Radiative Relaxation Quantum Yields for Synthetic Eumelanin, Photochem. Photobiol. 79 (2004) 211-216.

[5] S.P. Nighswander-Rempel, J. Riesz, J. Gilmore and P. Meredith, A quantum yield map for synthetic eumelanin, J. Chem. Phys. 123 (2005) 194–901.

[6] E. Kwam, and R. M. Tyrrell, The role of melanin in the induction of oxidative DNA base damage by ultraviolet A irradiation of DNA or melanoma cells, J. Invest. Dermatol. 113 (1999) 209–213.

[7] Korytowski, W., Pilas, B., Sarna, T., and Kalyanaraman, B. Photoinduced generation of hydrogen peroxide and hydroxyl radicals in melanins. Photochem. Photobiol. 45 (1987) 185–190.

[8] S. Takeuchi, W. G. Zhang, K. Wakamatsu, S. Ito, V. J. Hearing, K. H. Kraemer and D. E. Brash, Melanin acts as a potent UVB photosensitizer to cause an atypical mode of cell death in murine skin, P. Natl. Acad. Sci. U.S.A. 101 (2004) 15076-15081.

[9] P. Meredith, B. J. Powell, J. Riesz, S. P. Nighswander-Rempel, M. P.

Pederson and E. G. Moore, Towards structure–property–function relationships for eumelanin. Soft Matter 2 (2006) 37–44.

[10] S. Ito, A Chemist's View of Melanogenesis, Pigment Cell Res. 16 (2003) 230–236.

[11] S. Ito, K. Wakamatsu, Chemistry of mixed melanogenesis--pivotal roles of dopaquinone, Photochem. Photobiol. 84 (2008) 582–592.

[12] S. Ito, K. Wakamatsu, Chemistry of mixed melanogenesis--pivotal roles of dopaquinone, Photochem. Photobiol. 84 (2008) 582–592.

[13] P. Meredith and T. Sarna, The physical and chemical properties of eumelanin, Pigm. Cell Res. 19 (2006) 572-594.

[14] T. Sarna, Properties and function of the ocular melanin—A photobiophysical view, J. Photochem. Photobiol. 12 (1992) 215-258.

[15] S. D. Simon, L. Hong and D. N. Peles, Insights into melanosomes and melanin from some interesting spatial and temporal properties, J. Phys. Chem. B 112 (2008) 13201-13217.

[16] Y. Liu, L. Hong, K. Wakamatsu, S. Ito, B. B. Adhyaru, C. Y. Cheng, C. R. Bowers and J. D. Simon, Comparisons of the structural and chemical properties of melanosomes isolated from retinal pigment epithelium, iris and choroid of newborn and mature bovine eyes, Photochem. Photobiol. 81(2005) 510-516.

[17] Y. Liu, V. R. Kempf, J. B. Nofsinger, E. E. Weinert, M. Rudnicki, K. Wakamatsu, S. Ito and J. D. Simon, Comparison of the structural and physical properties of human hair eumelanin following enzymatic or acid/base

extraction, Pigm. Cell Res. 16 (2003) 355-365.

[18] K. Y. Ju, Y. Lee, S. Lee, S. B. Park and J. K. Lee, Bioinspired Polymerization of Dopamine to Generate Melanin-Like Nanoparticles having an Excellent Free-Radical-Scavenging Property, Biomacromolecules 12 (2011) 625-632.

[19] D. R. Dreyer, D. J. Miller, B. D. Freeman, D.R. Paul and C. W. Bielawski, Elucidating the Structure of Poly(dopamine), Langmuir 28 (2012) 6428−6435.

[20] S. Hong, Y. S. Na, S. Choi, I.T. Song, W. Y. Kim and H. Lee, Non-Covalent Self-Assembly and Covalent Polymerization Co-Contribute to Polydopamine Formation, Adv. Funct. Mater. 22 (2012) 4711–4717.

[21] M. d'Ischia, A. Napolitano, V. Ball, C. T. Chen and M. J. Buehler, Polydopamine and Eumelanin: From Structure−Property Relationships to a Unified Tailoring Strategy, Acc. Chem. Res. 47 (2014) 3541−3550.

[22] C. T. Chen, V. Ball, J. J. de Almeida Gracio, M. K. Singh, V. Toniazzo, D. Rush and M. J. Buehler, Self-Assembly of Tetramers of 5,6-Dihydroxyindole Explains the Primary Physical Properties of Eumelanin: Experiment, Simulation, and Design, ACS Nano 7 (2013) 1524-1532.

[23] J. B. Nofsinger, Y. Liu and J. D. Simon, Aggregation of eumelanin mitigates photogenertion of reactive oxygen species, Free Radic Biol Med. 32 (2002) 720-730.

[24] L. Mosca, C. De Marco, M. Fontana and M. A. Rosei, Fluorescence properties of melanins from opioid peptides, Arch. Biochem. Biophys. 371 (1999) 63–69.

[25] P. Meredith and J. Riesz, Radiative Relaxation Quantum Yields for Synthetic Eumelanin, Photochem. Photobiol. 79 (2004) 211-216.

[26] X. H. Qu, L. J. Kirschenbaum and E. T. Borish, Hydroxyterephthalate as a Fluorescent Probe for Hydroxyl Radicals: Application to Hair Melanin, Photochem. Photobiol. 71 (2000) 307-313.

[27] C. F. Bournonville and J. C. Díaz-Ricci, Quantitative Determination of Superoxide in Plant Leaves Using a Modified NBT Staining Method, Phytochem Anal. 22 (2011) 268-271.

Appendix/Chapter 2

Cellular uptake and excretion of Melanin-like Nanoparticles (MelNps)

2.1 Abstract

We have studied the interaction with cells, especially uptake, sub-cellular distribution and excretion of Melanin-like Nanoparticles (MelNps). The amount of nanoparticles, inside the cells that is affected by both the concentration and incubation time, was measured by the absorbance of MelNps inside the cells. Long incubation time indicates MelNps is biocompatible and images by Bright field spectroscopy and DIC (differential interference contrast) confocal spectroscopy showed the behavior of MelNps inside the cells.

2.2 Introduction

The rapid development of nanotechnology has generated numerous nanomaterials which have characteristic are different from those of bulk material of same chemical composition. Foundation of nanotechnology research is based on the size and shape of the nanomaterials which have distinct optical, electrical and magnetic properties. Recently, diverse synthetic nanoparticles are focused on exploiting in various biological applications such as imaging, bio-sensing, cell tracking, gene delivery due to their size similar to that of biological molecules and structures [1-4].

Despite of increasing applications of nanoparticles as biological materials, understanding of cellular uptake and excretion mechanism of interactions between nanoparticles and biological systems at various levels has been remained incompletely [5,6,7]. This situation has caused a number of studies, using Silica, titania, gold nanoparticles and quantum dot such as CdSe and CdTe, in recent years to shed light on the molecular interactions involved in the biological behavior of nanoparticles [8-12].

Depending on the particle size and surface conditions, most nanoparticles can enter the cells through endocytosis, which is the process that cell membranes wrap around the particles and takes it into the cell, and endocytosed nanoparticles are found in membrane bound organelles in the cytoplasm. However, mechanism that the nanoparticles evolve inside the cells and excrete from the cell is seldom discussed. Various colorimetric assays are generally used to evaluation cytotoxicity of nanoparticles that give only final

stage judgement of cytotoxicity. Consequently, how they enter the cell, evolve inside the cells and eventually how they are excreted out of the cells are the prerequisite information for researchers to obtain before biological applications of nanoparticles.

Among a number of nanoparticles, melanin-like nanoparticles (MelNps), similar to polydopamine and its derivatives that produced by auto-oxidation of dopamine, is widely used in diverse fields of nanomaterials lately [13, 14]. However, the mechanism behind the interaction of polydopamine, and its hybrid materials with cells, have not been discussed before. Consequently, we have studied the interaction with cells, especially uptake, sub-cellular distribution and excretion of nanoparticles, by synthetic melanin model, MelNps, which were successfully synthesized in our group before [15]. MelNps are similar to the natural eumelanin in terms of photo-physical property, structural unit and morphological appearance and an appropriate synthetic model similar to polydopamine. MelNps have also dispersible in water as well as biological media that give advantages in particle uptake into cells. Good biocompatibility of MelNps enables us to treatment high concentrations. In this chapter, we have investigated the uptake, sub-cellular distribution and excretion of MelNps in live cells based on absorbance measurement of particles uptake into the cells and CLSM (confocal laser scanning microscopy).

2.3 Experimental section

Preparation of melanin-like nanoparticles (MelNps)

We dissolved 180 mg of dopamine hydrochloride (Aldrich Chemical) in 90 mL of the temperature stabilized deionized water at 50 ℃. Under vigorous stirring, 780 μL of 1 N NaOH solution was added to the dopamine hydrochloride solution. The color of solution changed yellow as soon as 1 N NaOH was added and gradually turned to dark black in an hour. The reaction was allowed to continue for an additional 4 h, after which melanin-like nanoparticles were collected by centrifugation (18,000 rpm, 15 min) and washed several times with deionized water. After large aggregated materials were removed by low speed centrifugation (4000 rpm), the final purified melanin-like nanoparticles were stored in deionized water.

Pegylation of MelNps

NH_4OH solution (28 wt %) was added to 10 mL MelNps dispersed solution concentration of 1 mg/mL to adjust the pH of the solution 9.5~10. To this solution, 50 mg of methoxy-poly (ethylene glycol)-thiol (mPEG-SH, 2 kDa, SunBio, Ahn-Yang, South Korea) was added and stir vigorously at least 1 hr. Surface modified MelNps were obtained by centrifugation (20000 rpm, 10 min) and washed with deionized water several times.

The effects of the MelNps concentration and the incubation periods

HeLa cells were obtained from American Type Culture Collection (ATCC, Manassas, VA) and cultured in RPMI 1640 (GIBCO, Invitrogen) supplemented with heat-inactivated 10 % FBS (fetal bovine serum, GIBCO, Invitrogen). HeLa cell lines were maintained in a humidified atmosphere of 5 % CO_2 at 37 ℃. Cells were cultured in 96 well plates at a density of 4×10^3 cells/well and were left for 24 h and 48 h after treatment with MelNps solution (200 μL, various concentrations). Absorbance measurement of endocytosed MelNPs by ELISA at 405 nm was carried out after wash out with PBS buffer solution for remove the remaining nanoparticles dispersed in supernatant. Uptake of MelNps was determined relative to the absorbance of untreated control cells.

Excretion of MelNps by measuring absorption of MelNps

Cells were cultured in 96 well plates at a density of 4×10^3 cells/well and were left for 24 h and 48 h after treatment with MelNps solution (200 μL, various concentrations). The supernatant of each well was then removed and wash out with phosphate-buffered-saline (PBS) for removal of remaining nanoparticles. Absorbance of endocytosed MelNps was measured and incubated again with Nps free medium for 2 days. Excretion of MelNps was determined relative to the absorbance of untreated control cells.

Observation of cellular uptaken nanoparticles based on confocal microscopy

Cells were cultured in cover glass dishes at a density of 3×10^3 cells/well and incubated after treatment with MelNps solution (300 μL of 200 μg/mL) for 2 days. After wash out with PBS, the cells were observed in a humidified atmosphere of 5 % CO_2 at 37 ℃ by DIC (differential interference contrast) mode of confocal microscopy.

2.4 Result and discussion

Cellular uptake of melanin-like nanoparticles (MelNps)

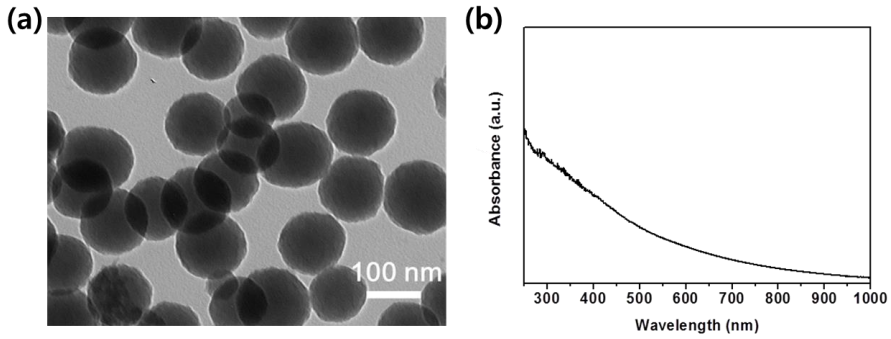

Figure 2-1. (a) TEM (transmission electron micromicroscopy) image and (b) UV-vis spectrum of melanin-like nanoparticles (MelNps).

TEM image of Melanin-like Nanoparticles (MelNps), which had already been successfully synthesized in our group before, as a synthetic eumelanin model similar to the natural eumelanin in terms of photo-physical property, structural unit and morphological appearance is in Figure 2-1 (a). The size of MelNps is approximately 100 nm that exhibits higher cellular uptake rate and greater distribution [16]. Good biocompatibility in HeLa cells as well as excellent dispersibility in aqueous and biological media is appropriate for cellular uptake experiments and broad band monotonic absorption in the region of UV-vis of melanin enables to observe the absorbance after nanoparticles' feeding.

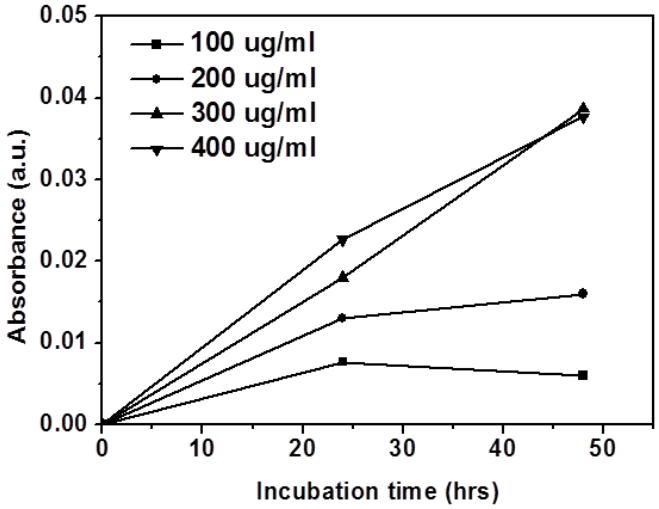

Figure 2-2. Absorbance of endocytosed MelNps dependent on concentration of particles and incubation time.

The effects of the MelNps concentration and the incubation periods were examined by incubating cells with concentration of 100, 200, 300, 400 μg/ml of MelNps for 24 h and 48 hr. Internalized nanoparticles were measured by the absorbance at 405 nm, the wavelength of strong absorption of MelNps. At higher concentration treatment of MelNps, at each incubation time, absorption intensity is higher which indicates that more MelNps are uptaken to the cells (Figure 2-2). It seems that internalization mechanism of MelNps is concentration-dependent at same incubation time.

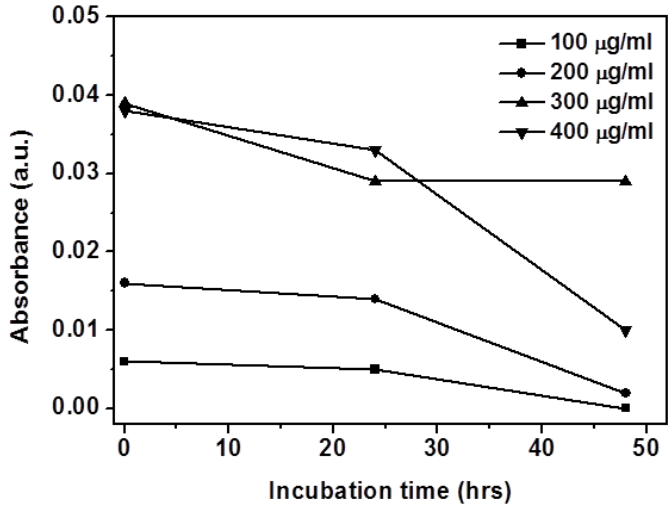

Figure 2-3. Absorbance decrement of endocytosed MelNps.

Excretion of nanoparticles was assessed by the decrement of absorbance from internalized MelNps during incubation with each concentration of MelNps for 48 hr. Incubated cells for 48 h with particles were washed out PBS buffer solution to remove the MelNps dispersed in the media and change to particle-free media for additional incubation for particle excretion. During the monitoring of excretion, washing out procedure was repeated at each incubation time for removal of excreted particles. Relatively low concentration of MelNps treated cells lose their absorbance at 405 nm faster than high concentration particle treated cells which have no absorbance only after 48 h incubation.

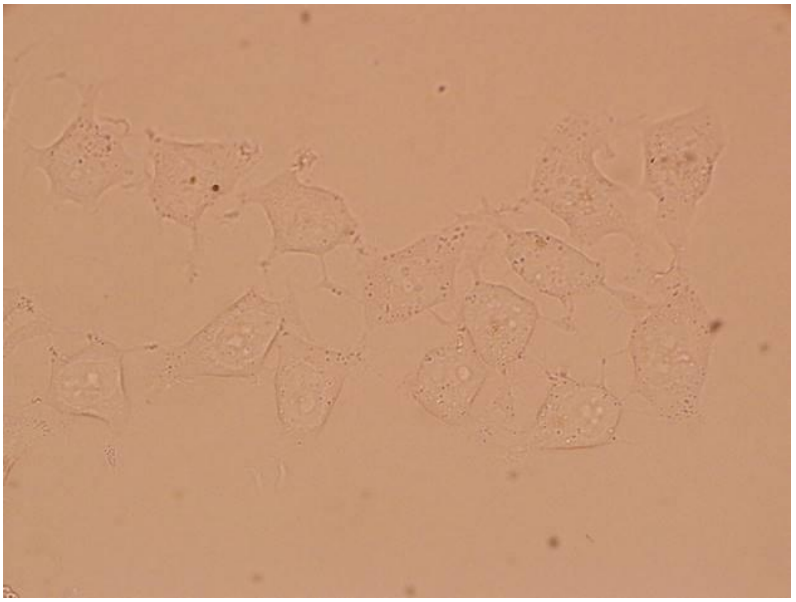

Figure 2-4. Bright field image of HeLa cells (200 μg/mL MelNps was treated for 48 h and washout with PBS to remove floating nanoparticles in the medium).

Cellular uptake and excretion of MelNps was also investigated with bright field spectroscopy. Even though the absorbance of cell at 405 nm increased after 48 h incubation with 200 μg/mL MelNps (Figure 2-2, Figure 2-3), there is no significant difference in the image of cells compared to the particle free incubated cells.

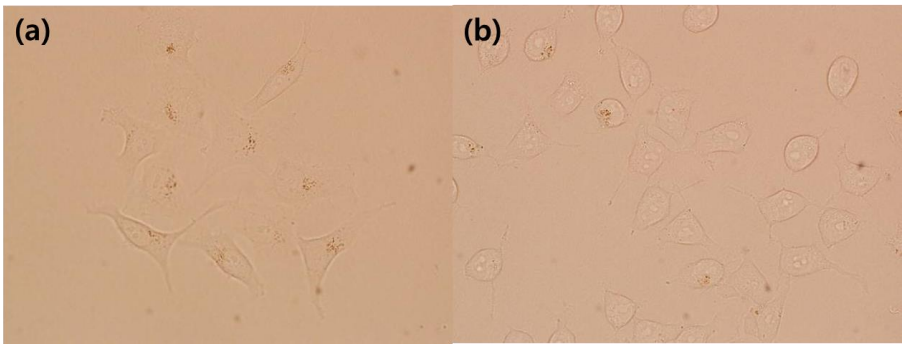

Figure 2-5. Bright field images of HeLa cells addition incubated in particle-free solution for (a) 24 h and (b) 48 h.

However, after 24 h incubation, clustering of dark dots appears in the cells in Figure 2-5 (a) and elongated of incubation times to 48 h, density and distribution of dark spots decreases (Figure 2-5 (b)). This tendency is consistent with the live images of cells recorded by DIC (differential interference contrast) mode of confocal microscopy in Figure 2-6.

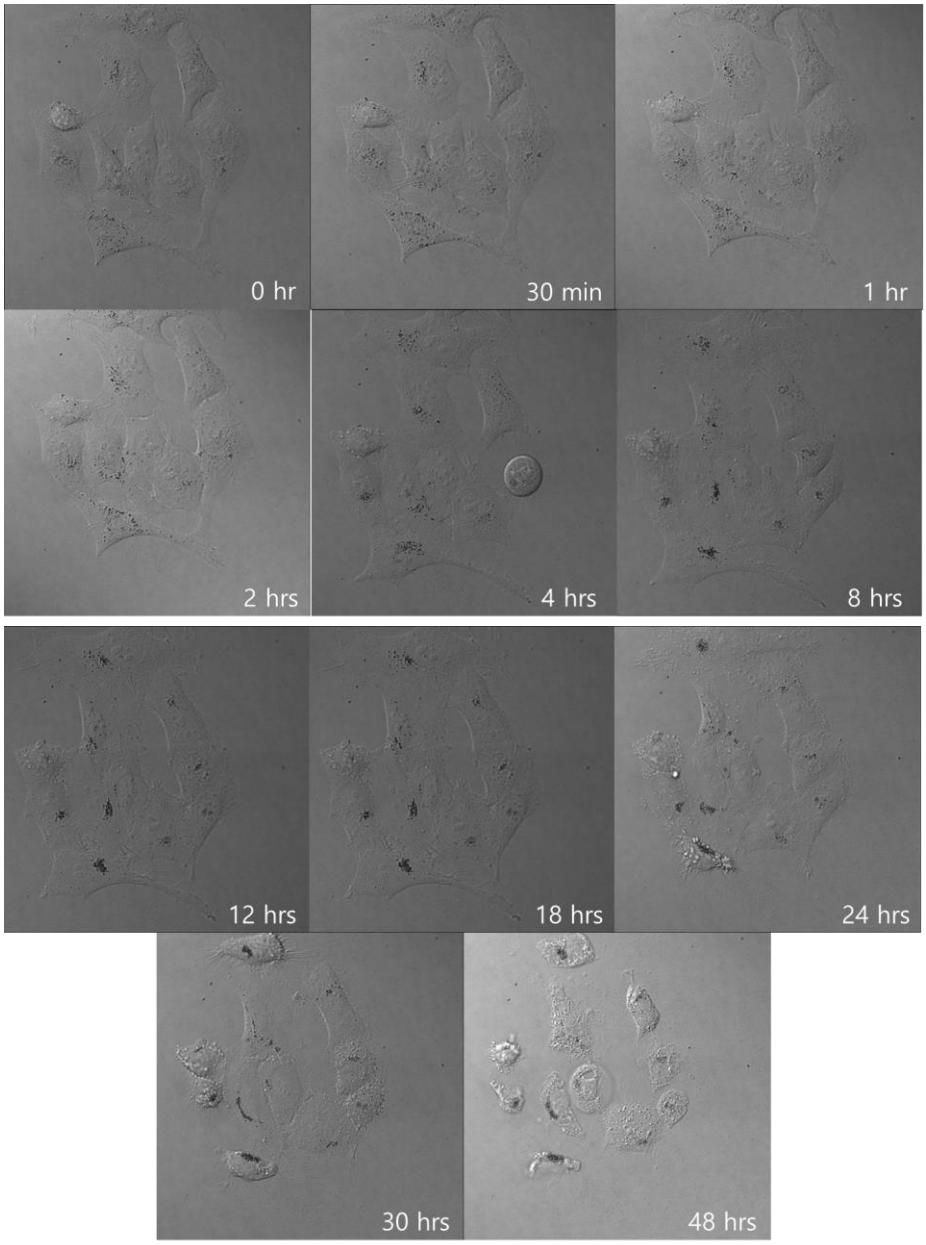

Figure 2-6. DIC images of live HeLa cells during incubation time.

DIC confocal spectroscopy was focused on one selected region and same cells to monitor of time-dependent evolution of endocytosed MelNps in live cells. It seems that most of MelNps uptaken into the cells are mono-dispersed

for short incubation time because clustering of particles emerges at longer incubation time. Interestingly, even after the progression of incubation times, MelNps are concentrated in the area of surrounding the nucleus. However, excretion of MelNps is elusive because of the limitation of magnification of apparatus even though the density of clustering nanoparticles and decrement absorption of particles inside the cells.

2.5 Conclusion

We have examined interaction between MelNps and cells. In particular, we have investigated the uptake, sub-cellular distribution and excretion of MelNps in live cells based on the confocal microscopy. The amount of MelNps inside the cells is affected by both the concentration of particles and feeding time. Even though the moment when endocytosis and exocytosis of particles was difficult to capture due to the limitation of resolution, clustering of particles and concentrated in the area of surrounding nucleus was observed. Also, there was no significant cytotoxicity of MelNps for a long incubation time at high concentration of particles.

2.6 Reference

[1] L. Latterini and M. Amelia, Sensing Proteins with Luminescent Silica Nanoparticles, Langmuir 25 (2009) 4767-4773.

[2] H. L. Lin, Y. S. Lin, H. Y. Lin, Y. Hung, L. W. Lo, Y. F. Chen and C. Y. Mou, In vitro Studies of Functionalized Mesoporous Silica Nanoparticles for Photodynamic Therapy, Adv. Mater. 21 (2009) 172–177.

[3] V. Vijayanathan, T. Thomas and T. J. Thomas, DNA Nanoparticles and Development of DNA Delivery Vehicles for Gene Therapy, Biochemistry 41 (2002) 14085-14094.

[4] B. Zhao, J. J. Yin, P. J. Bilski, C. F. Chignell, J. E. Roberts and Y. Y. He, Enhanced Photodynamic Efficacy towards Melanoma Cells by Encapsulation of Pc4 in Silica Nanoparticles, Toxicol. Appl. Pharmacol. 241 (2009) 163-172.

[5] In Vitro Cytotoxicitiy of Silica Nanoparticles at High Concentrations Strongly Depends on the Metabolic Activity Type of the Cell Line, Environ. Sci. Technol. 41(2007) 2064-2068.

[6] K. Kettler, K. Veltman, D. van de Meent, A. van Wezel, A. J. Hendriks, Cellular uptake of nanoparticles as determined by particle properties, experimental conditions, and cell type, Environ. Toxicol. Chem. 33 (2014) 481-492.

[7] T. Xia, M. Kovochich, M. Liong, L. Mädler, B. Gilbert, H. Shi, J. I. Yeh, J. I. Zink and A. E. Nel, Comparison of the Mechanism of Toxicity of Zinc Oxide and Cerium Oxide Nanoparticles Based on Dissolution and Oxidative

Stress Properties, ACS Nano 2 (2008) 2121-2134.

[8] B. D. Chithrani, W. C. W. Chan, Elucidating the Mechanism of Cellular Uptake and Removal of Protein-Coated Gold Nanoparticles of Different Sizes and Shapes, Nano Letters 7 (2007) 1542-1550.

[9] B. D. Chithrani, A. A. Ghazani, W. C. W. Chan , Determining the Size and Shape Dependence of Gold Nanoparticle Uptake into Mammalian Cells, Nano Letters 6 (2006) 662-668.

[10] J. Xie, C. Xu, N. Kohler, Y. Hou and S. Sun, Controlled PEGylation of Monodisperse Fe_3O_4 Nanoparticles for Reduced Non-Specific Uptake by Macrophage Cells, Adv. Mater. 19 (2007) 3163–3166.

[11] S. J. Cho, D. Maysinger, M. Jain, B. Ro¨der, S. Hackbarth and F. M. Winnik, Long-Term Exposure to CdTe Quantum Dots Causes Functional Impairments in Live Cells, Lanmuir 23 (2007) 1974-1980.

[12] R. E. Serda, A. Mack, M. Pulikkathara, A. M. Zaske, C. Chiappini, J. R. Fakhoury, D. Webb, B. Gobin, J. L. Conyers, X. W. Liu, J. A. Bankson and M. Ferrari, Cellular Association and Assembly of a Multistage Delivery System, Small 6 (2010) 1329-1340.

[13] M. d'Ischia, A. Napolitano, V. Ball, C. T. Chen and M. J. Buehler, Polydopamine and Eumelanin: From Structure−Property Relationships to a Unified Tailoring Strategy, Acc. Chem. Res. 47 (2014) 3541−3550.

[14] C. T. Chen, V. Ball, J. J. de Almeida Gracio, M. K. Singh, V. Toniazzo, D. Rush and M. J. Buehler, Self-Assembly of Tetramers of 5,6-Dihydroxyindole Explains the Primary Physical Properties of Eumelanin: Experiment,

Simulation, and Design, ACS Nano 7 (2013) 1524-1532.

[15] K. Y. Ju, Y. Lee, S. Lee, S. B. Park and J. K. Lee, Bioinspired Polymerization of Dopamine to Generate Melanin-Like Nanoparticles having an Excellent Free-Radical-Scavenging Property, Biomacromolecules 12 (2011) 625-632.

[16] J. Huang, L. Bu, K. Chen, Z. Cheng, X. Li and X. Chen, Effects of Nanoparticle Size on Cellular Uptake and Liver MRI with Polyvinylpyrrolidone-Coated Iron Oxide Nanoparticles, ACS Nano 4 (2010) 7151-7160.

.

Korean Abstract

자연계에 널리 분포하며 다양한 기능을 하는 멜라닌은 단백질과 같은 생체 분자들과는 다르게 분자구조에 대한 이해가 부족하여 정확한 구조가 알려지지 않은 생체 고분자이다. 멜라닌은 생체 내에서 합성 초기에 관여하는 특정 분자에 의해 eumelanin 과 pheomelanin 의 두 가지 종류로 합성이 진행되는 것으로 알려져 있고 단순히 색소로서의 역할 뿐만 아니라 항산화 작용, 자유 라디칼 억제 금속 이온 배위 등 다양한 생물학적 기능을 가지고 있다. 또한 자외선과 가시광선 전 영역의 흡수를 기반으로 높은 에너지의 전자기 복사선을 흡수하여 비활성화 시키는 광 보호 기능이 가장 잘 알려져 있고 그에 관한 많은 연구도 활발하게 진행되고 있는 반면, 이러한 이로운 생물학적 기능들과는 반대로 피부암이나 파킨슨씨 병과 같은 질병을 포함하여 강한 빛을 받았을 때 감광성을 나타내는 것 또한 멜라닌의 중요한 기능 중 하나이다.

이와 같은 멜라닌의 생물학적 특성들을 이해하기 위해서는 어떠한 구조적인 특성이 다양하고 상반되는 양상의 물리화학적 특성이나 생물학적 기능에 영향을 미치는지에 대한 이해가 필요한데 이제까지의 연구에 제안된 멜라닌 모델들은 생물학적 용매에 분산이 되지 않는 등 여러 한계를 가지고 있었고 특히 생체내의 멜라닌이 가지는 나노 입자 형태의 구조적 특성을 인공적인 합성방법으로는 재현하지 못하여 멜라닌의 독특한 물리화학적 특성과 생물학적 기능을 설명하는데 어려움이 있었다.

이러한 측면에서 이번 연구에서는 생체 멜라닌과 물리화학적 특성과 구조적 특징이 유사한 멜라닌 입자 모델들을 합성하고 이들을 이용하여

화학적으로 다르게 합성된 멜라닌의 물리화학적 특성을 비교 및 멜라닌 분석에 사용되는 화학적 산화를 기반으로 멜라닌의 구조변화와 그에 따른 물리화학적 특성 변화를 확인해보았다.

주요 핵심어: 유멜라닌, 페오멜라닌, 나노 입자 형태, 광감성, 산화에 따른 물리화학적 특성변화

학번: 2010-23103